US CLIVAR
VARIATIONS
doi: 10.5065/ybca-0s03
Fall 2021 • Vol. 19, No. 1

New frontiers for ocean surface currents

Guest Editors:
Kyla Drushka[1] and Mark Bourassa[2]

[1]University of Washington
[2]Florida State University

Ocean surface currents have a profound influence on human life through their role in horizontal transport and dispersal of pollutants and physical, biological, and chemical properties as well as in air-sea exchange of properties like heat and energy. Surface currents have been poorly observed, particularly within the upper meter of the ocean. Moreover, the vertical structure of currents within the upper ocean is not well understood, making it challenging to relate measurements and model estimates at different depths. While the OceanObs'99 meeting defined requirements for the surface current observing system as one measurement/month every 5x5 degrees, at 2 cm/s accuracy, the ocean and climate communities have since recognized the need to observe and model the highly energetic ocean variations found at smaller scales (kilometers to tens of kilometer and days to weeks). At the smallest of these scales (the submesoscale), near-surface convergence regimes and areas of horizontal gradients in currents lead to enhanced energy dissipation, vertical transport, and strong coupling between the ocean and the atmosphere. This is an emerging area of observational

Vertical structure of near-surface currents – Importance, state of knowledge, and measurement challenges

Shane Elipot[1] and Jacob Wenegrat[2]

[1]University of Miami
[2]University of Maryland, College Park

Importance

Near-surface currents are an expression of ocean dynamics within the air-sea transition zone, a key component of the climate system (Cronin et al. 2019). It is within this zone, of spatially and temporally evolving vertical extent, that the ocean and atmosphere constantly exchange kinetic and thermal energies, moisture, and gases including anthropogenic carbon dioxide.

The vertical scales over which ocean currents change speed and orientation from the surface, while still being relevant for air-sea processes, effectively defines the ocean side of the air-sea transition zone, or the oceanic boundary layer. This layer shares many dynamical characteristics with its counterpart, the atmospheric

IN THIS ISSUE

and modeling research that is constrained in part by the lack of velocity estimates at these scales. In coastal areas, high-resolution measurements are also a critical gap. Coupling between currents, waves, and wind is essential for air-sea momentum fluxes, particularly at strong winds, but uncertainties in observations and modeling these interactions remain. A number of recent technologies promise new advances in understanding surface currents, their vertical structure, and their interactions with waves and currents. These include drifters and buoys, airborne and satellite-based sensors measuring currents or sea surface height, in addition to other approaches and variables.

This edition of Variations follows the 2020 Surface Currents in the Coupled Ocean-Atmosphere System Workshop organized by US CLIVAR, which brought together 70 US and international participants with expertise in both the research and applications aspects of surface currents, including oceanography and atmospheric science, marine ecosystems and fisheries, and transport of plastics and oil. Contributed articles highlight the state of knowledge of vertical velocity structure and its implications and measurement challenges, wave-wind-current interactions, and the role of surface currents in biological dispersion. In addition, the expected impact of technological and modeling advances on scientific understanding of ocean forecasting is discussed.

US CLIVAR VARIATIONS

Editors:
Jennie Zhu and Mike Patterson
US CLIVAR Project Office
Washington, DC 20005
usclivar.org

boundary layer, but also differs in important ways due to the different impact of surface gravity waves. As such, observing and characterizing the vertical structure of near-surface currents is a pre-requisite for the fundamental understanding of the mechanics of climate at the air-sea interface. As an example, the flux of momentum into the ocean induced by the atmosphere, or wind stress, is a function of wind speed relative to the surface current speed (Chelton et al. 2004). As a result, estimating wind energy input using any other estimate of ocean current than at the surface will be biased if the vertical structure of these currents is significant (Elipot and Gille 2009b; Liu et al. 2019), yet the meaning of “surface” here, or for other applications, is not always clearly defined.

Near-surface currents lead to the drift and dispersion of all suspended animate and inanimate matter. From the macro to the micro scales, the temporal and the three-dimensional spatial distribution of marine life is conditioned by the vertical penetration of sunlight and species-specific ranges of depths over which vertically-varying currents and turbulence interact with biogeochemical processes (Lévy et al. 2018). Near-surface currents constitute the most important variable (among for example winds, waves, and sea surface temperature) that needs to be modeled to accurately predict the fate of pollutants that threaten ecosystem and human health such as plastics, oil spills, radioactive isotopes, and chemical compounds (Röhrs et al. 2021). While pollutants typically enter the ocean at the air-sea interface, vertical mixing and current shear determine how far and at which depths they will travel (van Sebille et al. 2018), and accurate prediction requires integration of near-surface currents over the vertical extent of floating and suspended objects (Olascoaga et al. 2020). Knowledge of currents at a single-depth is not sufficient. Even observations close to the surface show significant shear within a few centimeters from the air-sea interface (Laxague et al. 2018). Knowledge of near-surface currents is also an important component of saving lives at sea through search-and-rescue operations, which requires successful modeling of near-surface currents and appropriate depth-dependent observations for validation. Therefore it can be concluded that the knowledge and high modeling skill of the vertical structure of near-surface currents is relevant to achieve appropriate national and international management of marine resources and hazards (Röhrs et al. 2021), and thus contribute to several of the planned outcomes of the ongoing UN Decade of Ocean Science for Sustainable Development that include a productive, predicted, and safe ocean (UNESCO-IOC 2021).

Ekman theory, one of the pillars of dynamical oceanography, provides us with the mechanism by which the oceanic general circulation is forced by the so-called Ekman pumping vertical velocity, which drives changes in sub-surface density fields and pressure gradients. Ekman theory further indicates that details of the vertical distribution of wind-induced stress within the boundary layer are irrelevant for determining Ekman pumping velocities. Yet, these details are critical to the vertical structure of the near-surface Ekman currents, the vertical fluxes of momentum, the dissipation of wind energy within the oceanic boundary layer (Elipot and Gille 2009a,b; Alford 2020), and the associated vertical mixing of upper ocean properties, including the upper ocean heat content distribution and sea surface temperature variability. As such, the vertical structure of Ekman currents remains an active area of research well over a century after its formulation.

Despite their importance, the definition of surface currents, or near-surface currents, and how this definition is related to their vertical structure is not clearly established (Röhrs et al. 2021). This is in contrast to sea surface temperature, another near-surface ocean property whose vertical structure has been the focus of international efforts and coordination by the Group for High Resolution Sea Surface Temperature (Donlon et al. 2009). Under the sponsorship of the World Meteorological Organization and the IOC-UNESCO, the Global Climate Observing System defined surface currents as one of the 54 Essential Climate Variables (ECV) that critically contributes to the characterization of Earth's climate. In parallel, the Global Ocean Observing System (GOOS) and the World Climate Research Program support the Ocean Observations Physics and Climate Panel (2017) which defined surface currents as one of the key physical Essential Ocean Variables (EOV) that are effectively addressing the overall GOOS themes of climate, operational ocean services, and ocean health. For both classifications, as an ECV or an EOV, the relevant specification sheets of surface currents specify that a depth must be stated when dealing with this variable, effectively recognizing the importance of its vertical structure.

In summary, the vertical structure of near-surface currents is of relevance for a wide range of multidisciplinary scientific research and operational applications whose successes can only grow as oceanographers expand their state of knowledge.

State of knowledge

The dynamical processes responsible for near-surface shear include thermal wind flow, wind-driven Ekman currents, surface gravity waves, and ageostrophic flows associated with submesoscale fronts. The conceptual understanding of these processes is grounded in well-developed theories, however major gaps exist in the details. Persistent challenges remain towards determining the temporal variability of shear and rectification across timescales, the detailed structure of shear flow very near the sea-surface, and the interaction between the various dynamical sources of shear-flow (e.g., wave-current interactions, the subject of another article in this issue). Understanding is further complicated by the fact that turbulent momentum fluxes are often both a leading-order term in the dynamics of near-surface shear flows, and are in turn affected by the sheared flow through buoyancy advection and shear production of turbulent kinetic energy. These gaps in the "details" are often not well captured by observations nor represented in numerical models, and they stand as major challenges for operational oceanography, instrument cross-calibration, and model development.

In ocean general circulation models where surface gravity waves are not included and submesoscale fronts are generally not resolved, the broad spatial pattern of surface shear is dominated by the response to the surface wind forcing (Figure 1). Time-varying winds generate shear near the surface over a vertical scale that is dependent on the forcing frequency (Gonella 1971; Elipot and Gille 2009a; Lilly and Elipot 2021), and with vertical structure that depends on the profile of turbulent momentum flux (Madsen 1977; Miles 1994; Wenegrat and McPhaden 2016a), a challenging quantity to resolve in observations. Surface gravity waves further complicate the basic conceptual picture of wind-driven shear, both as an additional source of near-surface shear (which often dominates the directly wind-forced shear flow) (Belcher et al. 2012) and through new terms in the Eulerian wave-averaged momentum equations. This includes the Stokes-Coriolis term, which can be a leading-

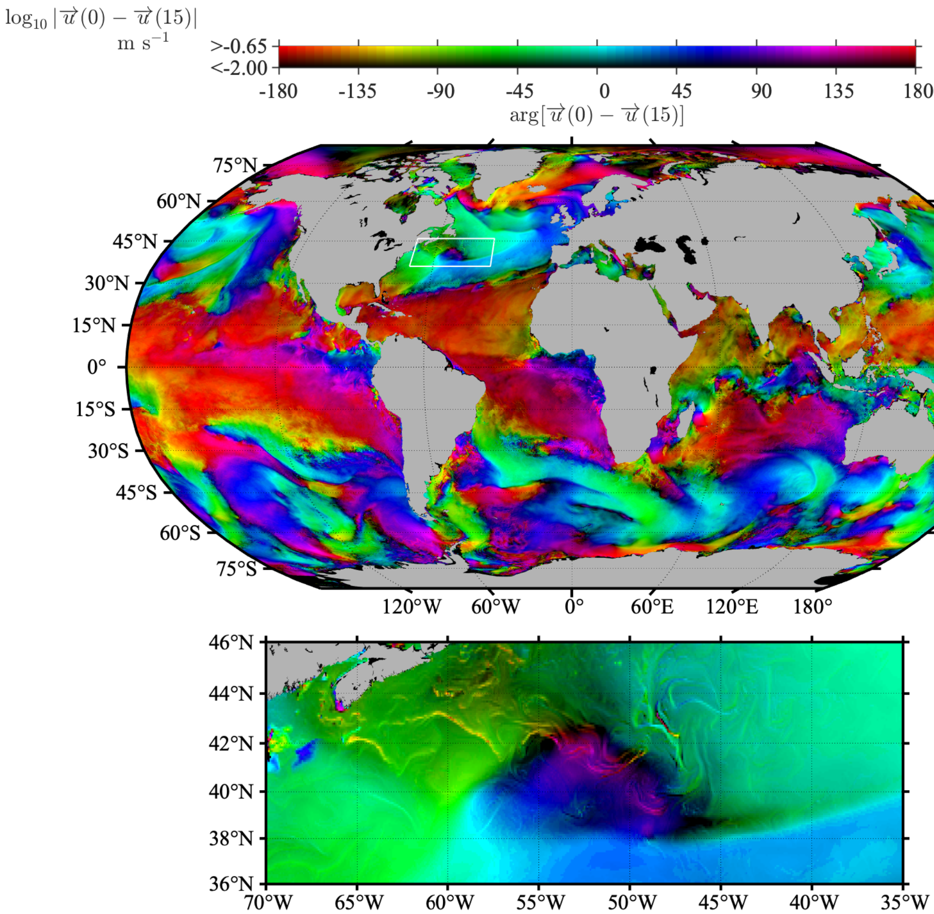

Figure 1. Snapshot of near-surface currents shear in the HYbrid Coordinate Ocean Model (HYCOM). This figure displays the velocity at 0 m minus the velocity at 15 m in a run of HYCOM at approximately 1/25 degree resolution on January 1, 2014 (Arbic et al. 2010). The outputs from the model were first regridded on a regular 2/25 degree uniform grid. The lower panel is a zoom on the region delineated in the upper panel by a white rectangle in the North Atlantic. The velocity difference is indicated using a Hue-Saturation-Value (HSV) color model with a constant color saturation of one as indicated by the colorbar. The color hue indicates the angle difference (positive counterclockwise), and the color value indicates the decimal logarithm of the absolute value of the difference from less than 0.01 m s^{-1} (black) to more than 0.22 m s^{-1} (full value).

order modification to the classic Ekman solutions (Huang 1979; Polton et al. 2005), and a Stokes-vortex force term, central to the generation of Langmuir circulation. Velocity shear can be further modified by surface wave effects on turbulence through the Stokes shear production and enhanced downward transport of turbulent kinetic energy (McWilliams et al. 1997; D'Asaro 2014; Li and Fox-Kemper 2017). Despite recent developments of turbulence parameterizations that aim to include the effects of surface waves on turbulence (Li et al. 2019; Chor et al. 2021), the Stokes drift and wave effects on currents are still absent from many ocean simulations, limiting their applicability to problems in Lagrangian dispersal (Fraser et al. 2018; van Sebille et al. 2020).

Interactions between dynamics and the buoyancy field are also critical to the wind-driven response. Stratification inhibits the vertical transport of momentum, thus generating strong inertial shear across the mixed-layer base. Time-varying stratification near the surface leads to the formation of thin shear layers, such as the afternoon diurnal jet (Price et al. 1986; Cronin and Kessler 2009),

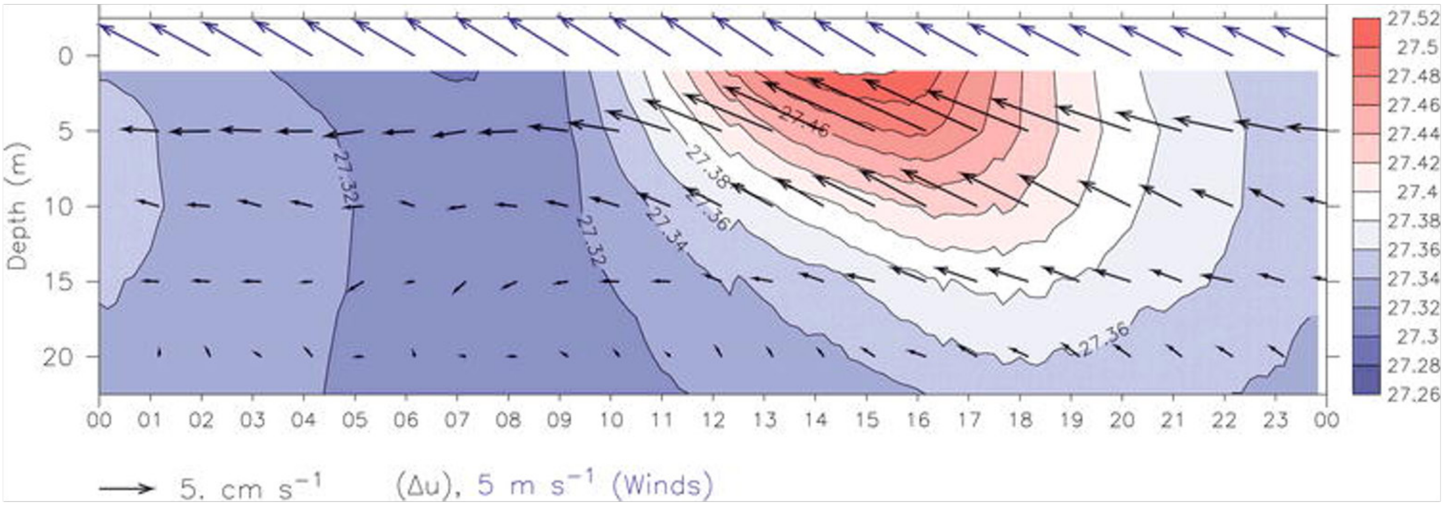

Figure 2. A composite diurnal cycle of shear flow from approximately 4 months of moored observations at 2°N, 140°W in the tropical Pacific. Observed currents are shown (black vectors) referenced to 25 m depth, oriented such that northward vectors point up, eastward vectors point right. The surface wind is also shown (blue vectors). Afternoon near-surface warming (temperature, colorscale) leads to the development of stratification that inhibits the downward transport of momentum from the surface, accelerating a sheared diurnal jet in the downwind direction. Figure from Cronin and Kessler 2009.

where afternoon surface heating leads to the development of near-surface stratification, a concomitant reduction in turbulent momentum transfer away from the surface, and the acceleration of a sheared jet in the downwind direction (Figure 2). The presence of these fast-timescale shear flows is known to drive turbulent mixing in the tropics (Moum and Caldwell 1985; Lien et al. 1995; Smyth et al. 2013; Wenegrat and McPhaden 2015), to rectify to affect the vertical structure of low-frequency shear flows (McWilliams et al. 2009; Wenegrat and McPhaden 2016b), and to affect climate variability on intraseasonal and longer timescales (Shinoda 2005; Danabasoglu et al. 2006; Bernie et al. 2007, 2008). Current generation models are capable of capturing these processes and interactions if run with sufficiently high vertical resolution and when considering regions of relative spatial homogeneity (where turbulence parameterizations are well-vetted). These conditions are not always met because they are computationally expensive and because much of the world's oceans contain significant horizontal variability.

Horizontal buoyancy gradients, or fronts, are regions of strong shear flow, both through the well-known thermal wind balance and through other ageostrophic frontal dynamics at the submesoscale, which are not as completely understood (McWilliams 2016). For example, the Gulf Stream region in Figure 1 shows stripes of high-shear regions associated with both persistent large-scale fronts, such as the western boundary current, and transient mesoscale eddies present in this 1/25° HYCOM simulation. Observations indicate the surface buoyancy power spectrum has an approximately k^{-2} horizontal wavenumber slope down to much smaller scales (Ferrari and Rudnick 2000) with strong thermal wind shear present through the submesoscale (below the resolution of this simulation). At these small scales, loss of balance occurs through a variety of frontal processes (McWilliams 2016), and sharp fronts are sites of both strong thermal wind and ageostrophic shear. Processes at this scale tend to evolve quickly (on the order of hours) and are sensitive to the time-varying surface forcing (Thomas et al. 2016; Duahajre et al. 2018; Sun et al. 2020). At the same time, boundary layer turbulence is also strongly modulated at fronts by the advection of buoyancy and the extraction of kinetic energy from the balanced flow by the geostrophic shear production (Taylor and Ferrari

2010; D'Asaro et al. 2011; Thomas et al. 2016; Smith et al. 2016). Sharp fronts in the surface boundary layer thus lead to coupled interactions between frontal dynamics, turbulence, and the wind-driven flow, which modify the near-surface shear flow through a variety of pathways that have not yet been fully explored. For example, the Ekman transport is modified by the vertical relative vorticity (Niiler 1969; Wenegrat and Thomas 2017), and inertial oscillations at fronts can have significant ellipticity and vertical shear (Whitt and Thomas 2015; Skyllingstad and Samelson 2020). This is in contrast to the predictions of classic slab-layer conceptual models, and has been shown to increase horizontal tracer dispersion (Wenegrat et al. 2020). Determining to what extent these intense, but spatially localized, sources of frontal shear flow matter to larger-scale circulation, tracer dispersion, and climate remains an important priority for improved modeling and prediction.

Measurement challenges and future outlook

Complete observations of the vertical structure of near-surface currents requires continuous sampling of the water column downward from the oscillating air-sea interface. Fully understanding these observations further requires apprehending environmental conditions such as density stratification and atmospheric forcings. Eulerian observations from moorings form an important basis of our observations of near-surface velocity and are well-suited to simultaneous collection of velocity, temperature, salinity, and meteorological data. Current meters deployed at fixed depths on mooring lines or surface buoys can capture both spatial and temporal structure of near-surface currents (Weller and Pluddemann 1996; Farrar and Weller 2006). However, these observations are often limited in vertical resolution and when made close to the surface, can suffer from biases due to mooring motions induced by surface gravity waves (Pollard 1973; Rascle and Ardhuin 2009). Acoustic Doppler Current Profilers (ADCPs) can also be mounted on moorings, either in a subsurface upward-facing configuration or in a downward facing configuration attached to surface moorings, providing well-resolved vertical profiles. Both configurations can, however, suffer from signal contamination from various sources, including surface gravity waves, such that the upper few meters of the water column are often not resolved, and fish, which aggregate under surface moorings, causing low biases in ADCP velocity magnitudes.

Alternate measurement techniques focus on near-surface Lagrangian currents, traditionally achieved by observing the drift of floating objects that are advected by total currents, that is the currents that are the result of all geophysical processes and their interactions (Rörhs et al. 2021; Marié et al. 2020). The water-following characteristics of a floating object are a function of the object's combined geometry and buoyancy, impacted by the direct force applied by near-surface winds if the object is partially exposed to air and the vertical structure of near-surface currents over the vertical extent of the object (Olascoaga et al. 2020). Drift measurements are now relatively abundant thanks to the drifting buoys, or drifters, of the NOAA Global Drifter Program (GDP, Lumpkin and Pazos 2007), which are initially drogued to follow currents at 15 m depth. GDP observations have allowed the characterization of near-surface currents arising from both the low-frequency and large-scale oceanic global circulation (Laurindo et al. 2018) and high-frequency and small scales processes including internal waves (Elipot and Lumpkin 2008; Elipot et al. 2016; Poulain and Centurioni 2015; Yu et al. 2019; Zaron and Elipot 2020). The preponderance of near-surface current observations from the GDP has had a large influence on our view of what constitutes the near-surface oceanic circulation. The majority of GDP ocean current observations actually originate from "undrogued drifters'' that have lost their anchor, the water-following capabilities of which are not completely known (Laurindo et al. 2018). Systematic comparisons between drogued and undrogued drifter data may be an underutilized source of information on near-surface shear. Drifters with designs that differ from those of the GDP have also been deployed for a number of dedicated process studies (Poje et al. 2014). However, combining drifters of different designs introduces uncertainty due to differing water-following capabilities and biases (Lumpkin et al. 2017). The influence of various geophysical processes on comparisons between drifter types is not yet fully understood, and comparisons between simulated drogued and undrogued surface drifters using a tide-simulating run of the MITgcm indicate average differences that depend on both frequency and latitude (Yu et al. 2019).

The spatial variability of near-surface currents can also be measured by remote sensing observations, but capturing remotely the current shear is more difficult. For example, the geostrophic component of near-surface currents is regularly obtained from satellite-borne altimetric radar instruments measuring sea surface height, but the thermal wind shear component can only be obtained from ancillary in situ data. Along coastal areas, high frequency radars provide estimates of the velocity of that upper layer of the ocean that interacts with small surface gravity waves. Yet, the nature of the surface currents estimated in this way (Eulerian or Langrangian) and the depth scale that they represent, are still a topic of active discussion (Isern-Fontanet et al. 2017). Comparisons with other current measurements lead to results that appear to depend on environmental conditions (Röhrs and Christensen 2015).

The distinct capabilities, as well as limitations, of the various instrumental platforms mentioned above altogether suggest that a successful strategy to measure the vertical structure of near-surface currents will need to include integrations and syntheses of different types of observations in parallel with theory advancements and numerical modeling to aid interpretations. Examples of such successes that have managed to obtained shear measurements extremely close to the surface include the combination of microstructure profiler, ADCPs, and surface gravity wave measurements (Sutherland et al. 2016), and the combination of various drifters, imaging techniques, and ADCPs (Laxague et al. 2018). There is currently a range of proposed satellite missions aiming at measuring simultaneously a mixture of surface currents, atmospheric winds, and surface gravity waves (Ardhuin et al. 2018; Rodriguez et al. 2018; Ardhuin et al. 2019; Chelton et al. 2019; Rodriguez et al. 2019; Villas Bôas et al. 2019) for which calibration and validation efforts will be of the utmost importance; not only to acquire accurate estimates of currents at the surface but also potentially to understand how these relate to currents just below the surface. Combining observations necessitates understanding both the potential uncertainties associated with individual measurements and how the spatial heterogeneity and non-stationarity of oceanic processes near the surface may conflate the horizontal and vertical shears of near-surface currents.

Acknowledgments

SE was supported by NSF Award 1851166. JOW was supported by NASA award 80NSSC21K0554.

References

Alford, M. H., 2020: Revisiting near-inertial wind work: Slab models, relative stress, and mixed layer deepening. *J. Phys. Oceanogr.*, **50**, 3141-3156, doi:10.1175/JPO-D-20-0105.1.

Arbic, B. K., A. J. Wallcraft, and E. J. Metzger, 2010: Concurrent simulation of the eddying general circulation and tides in a global ocean model. *Ocean Model*., **32**, 175-187, doi:10.1016/j.ocemod.2010.01.007.

Ardhuin, F, and Coauthors, 2018: Measuring currents, ice drift, and waves from space: The Sea surface KInematics Multiscale monitoring (SKIM) concept. *Ocean Sci.*, **14**, 337-354, doi:10.5194/os-14-337-2018.

Ardhuin, F., and Coauthors, 2019: Satellite Doppler observations for the motions of the oceans. *Bull. Amer. Meteor.Soc.*, **100**, ES215-ES219, doi:10.1175/BAMS-D-19-0039.1.

Belcher, S. E., and Coauthors, 2012: A global perspective on Langmuir turbulence in the ocean surface boundary layer. *Geophys. Res. Lett.*, **39**, doi:10.1029/2012GL052932.

Bernie, D. J., E. Guilyardi, G. Madec, J. M. Slingo, and S. J. Woolnough, 2007: Impact of resolving the diurnal cycle in an ocean atmosphere GCM. Part 1: A diurnally forced OGCM. *Climate Dyn*., **29**, 575–590, doi:10.1007/s00382-007-0249-6.

Bernie, D. J., E. Guilyardi, G. Madec, J. M. Slingo, S. J. Woolnough, and J. Cole, 2008: Impact of resolving the diurnal cycle in an ocean atmosphere GCM. Part 2: A diurnally coupled CGCM. *Climate Dyn*., **31**, 909–925, doi:10.1007/s00382-008-0429-z.

Chelton, D. B., M. G. Schlax, M. H. Freilich, and R. F. Milliff, 2004: Satellite measurements reveal persistent small-scale features in ocean winds. *Science*, **303**, 978-983, doi:10.1126/science.1091901.

Chelton, D. B., M. G. Schlax, R. M. Samelson, J. T. Farrar, M. J. Molemaker, J. C. McWilliams, and J. Gula, 2019: Prospects for future satellite estimation of small-scale variability of ocean surface velocity and vorticity. *Prog. Oceanogr*., **173**, 256-350, doi:10.1016/j.pocean.2018.10.012.

Chor, T., J. C. McWilliams, and M. Chamecki, 2021: Modifications to the *K*-profile parameterization with nondiffusive fluxes for Langmuir turbulence. *J. Phys. Oceanogr.*, **51**, 1503–1521, doi:10.1175/JPO-D-20-0250.1.

Cronin, M. F., and W. S. Kessler, 2009: Near-surface shear flow in the tropical Pacific cold tongue front. *J. Phys. Oceanogr.*, **39**, 1200–1215, doi:10.1175/2008JPO4064.1.

Cronin, M. F., and Coauthors, 2019: Air-sea fluxes with a focus on heat and momentum. *Front. Mar. Sci*., **6**, doi:10.3389/fmars.2019.00430.

D'Asaro, E. A., C. Lee, L. Rainville, R. Harcourt, and L. Thomas, 2011: Enhanced turbulence and energy dissipation at ocean fronts. *Science*, **332**, 318–322, doi:10.1126/science.1201515.

D'Asaro,E. A., J. Thomson, A. Y. Shcherbina, R. R. Harcourt, M. F. Cronin, M. A. Hemer, and B. Fox-Kemper, 2014: Quantifying upper ocean turbulence driven by surface waves. *Geophys. Res Lett.*, **41**, 102–107, doi:10.1002/2013GL058193.

Danabasoglu, G., W. G. Large, J. J. Tribbia, P. R. Gent, B. P. Briegleb, and J. C. McWilliams, 2006: Diurnal coupling in the tropical oceans of CCSM3. *J Climate*, **19**, 2347–2365, doi:10.1175/JCLI3739.1.

Donlon, C. J., and Coauthors, 2009: The GODAE high-resolution sea surface temperature pilot project. *Oceanography*, **22**, 34–45. doi:10.5670/oceanog.2009.64.

Dauhajre, D. P., and J. C. McWilliams, 2018: Diurnal evolution of submesoscale front and filament circulations. *J. Phys. Oceanogr.*, **48**, 2343–2361, doi:10.1175/JPO-D-18-0143.1.

Elipot, S., and S. T. Gille, 2009a: Ekman layers in the Southern Ocean: Spectral models and observations, vertical viscosity and boundary layer depth. *Ocean Sci*., **5**, 115-139, doi:10.5194/os-5-115-2009.

Elipot, S., and S. T. Gille, 2009b: Estimates of wind energy input to the Ekman layer in the Southern Ocean from surface drifter data. *J. Geophys. Res.: Oceans*, **114**, doi:10.1029/2008JC005170.

Elipot, S. and R. Lumpkin, 2008: Spectral description of oceanic near-surface variability. *Geophys. Res. Lett.*, **35**, doi:10.1029/2007GL032874.

Elipot, S., R. Lumpkin, R. C. Perez, J. M. Lilly, J. J. Early, and A. M. Sykulski, 2016: A global surface drifter data set at hourly resolution. *J. Geophys. Res.: Oceans*, **121**, 2937-2966, doi:10.1002/2016JC011716.

Farrar, J. T., and R. A. Weller, 2006: Intraseasonal variability near 10°N in the eastern tropical Pacific Ocean. *J. Geophys. Res.: Oceans*, **111**, doi:10.1029/2005JC002989.

Ferrari, R., and D. L. Rudnick, 2000: Thermohaline variability in the upper ocean. *J. Geophys. Res.: Oceans*, **105**, 16857–16883, doi:10.1029/2000JC900057.

Fraser, C. I., and Coauthors, 2018: Antarctica's ecological isolation will be broken by storm-driven dispersal and warming. *Nat. Climate Change*, **8**, 704–708, doi:10.1038/s41558-018-0209-7.

Gonella, J., 1971: A local study of inertial oscillations in the upper layers of the ocean. *Deep Sea Res. Oceanogr. Abstr.*, **18**, 775–788, doi:10.1016/0011-7471(71)90045-3.

Huang, N. E., 1979: On surface drift currents in the ocean. *J. Fluid Mech.*, **91**, 191-208, doi:10.1017/S0022112079000112.

Isern-Fontanet, J., J. Ballabrera-Poy, A. Turiel, and E. García-Ladona, 2017: Remote sensing of ocean surface currents: A review of what is being observed and what is being assimilated. *Nonlinear Processes Geophys*., **24**, 613-643, doi:10.5194/npg-24-613-2017.

Laurindo, L. C., A. J. Mariano, and R. Lumpkin, 2017: An improved near-surface velocity climatology for the global ocean from drifter observations. *Deep Sea Res. Part I*, **124**, 73-92, doi:10.1016/j.dsr.2017.04.009.

Laxague, N. J., and Coauthors, 2018: Observations of near-surface current shear help describe oceanic oil and plastic transport. *Geophys. Res. Lett.*, **45**, 245-249, doi:10.1002/2017GL075891.

Lévy, M., P. J. Franks, and K. Shafer Smith, 2018: The role of submesoscale currents in structuring marine ecosystems. *Nat. Commun.*, **9**,doi:10.1038/s41467-018-07059-3.

Li, Q., and B. Fox-Kemper, 2017: Assessing the effects of Langmuir turbulence on the entrainment buoyancy flux in the ocean surface boundary layer. *J. Phys. Oceanogr.*, **47**, 2863– 2886, doi:10.1175/JPO-D-17-0085.1.

Li, Q., and Coauthors, 2019: Comparing ocean surface boundary vertical mixing schemes Including Langmuir turbulence. *J. Adv. Model. Earth Syst.*, **11**, 3545–3592, doi:10.1029/2019MS001810.

Lien, R.-C., D. R. Caldwell, M. C. Gregg, and J. N. Moum, 1995: Turbulence variability at the equator in the central Pacific at the beginning of the 1991-1993 El Niño. *J. Geophys. Res.*, **100**, 6881-6898, doi:10.1029/94JC03312.

Lilly, J. M., and S. Elipot, 2021: A unifying perspective on transfer function solutions to the unsteady Ekman problem. *Fluids*, **6**, doi:10.3390/fluids6020085.

Liu, Y., Z. Jing, and L. Wu, 2019: Wind power on oceanic near-inertial oscillations in the global ocean estimated from surface drifters. *Geophys. Res. Lett.*, **46**, 2647-2653, doi:10.1029/2018GL081712.

Lumpkin, R, T. Özgökmen and L. Centurioni, 2017: Advances in the application of surface drifters. *Annu. Rev. Mar. Sci*., **9**, 59-81, doi:10.1146/annurev-marine-010816-060641.

Lumpkin, R., and M. Pazos, 2007: Measuring surface currents with SVP drifters: The instrument, its data, and some recent results. *Lagrangian Analysis and Prediction of Coastal and Ocean Dynamics*, A. Griffa, A. D. Kirwan, Jr., A. J. Mariano, T. Özgökmen, and H. T. Rossby, Eds., Cambridge Univ. Press, 39–67.

Marié, L., and Coauthors, 2020: Measuring ocean total surface current velocity with the KuROS and KaRADOC airborne near-nadir Doppler radars: A multi-scale analysis in preparation for the SKIM mission. *Ocean Sci*., **16**, 1399-1429, doi:10.5194/os-16-1399-2020.

Madsen, O. S., 1977: A realistic model of the wind-induced Ekman boundary layer. *J. Phys. Oceanogr.*, **7**, 248–255, doi:10.1175/1520-0485(1977)007<0248:ARMOTW>2.0.CO;2.

McWilliams, J. C., 2016: Submesoscale currents in the ocean. *Proc. R. Soc. A*, **472**, doi:10.1098/rspa.2016.0117.

McWilliams, J. C., E. Huckle, and A. F. Shchepetkin, 2009: Buoyancy effects in a stratified Ekman layer. *J. Phys. Oceanogr.*, **39**, 2581–2599, doi:10.1175/2009JPO4130.1.

McWilliams, J. C., P. P. Sullivan, and C.-H. Moeng, 1997: Langmuir turbulence in the ocean. *J. Fluid Mech.*, **334**, 1–30, doi:10.1017/S0022112096004375.

Miles, J., 1994: Analytical solutions for the Ekman layer. *Boundary-Layer Meteor.*, **67**, 1–10, doi:10.1007/BF00705505.

Moum, J. N., and D. R. Caldwell, 1985: Local Influences on shear-flow turbulence in the equatorial ocean. *Science*, **230**, 315–316, doi:10.1126/science.230.4723.315.

Niiler, P. P., 1969: On the Ekman divergence in an oceanic jet. *J. Geophys. Res.*, **74**, 7048-7052, doi:10.1029/JC074i028p07048.

Olascoaga, M. J., F. J. Beron-Vera, P. Miron, J. Triñanes, N. F. Putman, R. Lumpkin, and G. J. Goni, 2020: Observation and quantification of inertial effects on the drift of floating objects at the ocean surface. *Phys. Fluids*, **32**, doi:10.1063/1.5139045.

Poje, A.C., and Coauthors, 2014: Submesoscale dispersion in the vicinity of the Deepwater Horizon spill. *Proc. Natl. Acad. Sci.*, **111**, 12693-12698, doi:10.1073/pnas.1402452111.

Pollard, R., 1973: Interpretation of near-surface current meter observations. *Deep Sea Res. Oceanogr. Abstr.*, **20**, doi:10.1016/0011-7471(73)90015-6.

Polton, J. A., D. M. Lewis, and S. E. Belcher, 2005: The role of wave-induced Coriolis-Stokes forcing on the wind-driven mixed layer. *J. Phys. Oceanogr.*, **35**, 444–457, doi:10.1175/JPO2701.1.

Poulain, P.-M., and L. Centurioni, 2015: Direct measurements of world ocean tidal currents with surface drifters. *J. Geophys. Res.: Oceans*, **120**, 6986–7003, doi:10.1002/2015JC010818.

Price, J. F., R. A. Weller, and R. Pinkel, 1986: Diurnal cycling: Observations and models of the upper ocean response to diurnal heating, cooling, and wind mixing. *J. Geophys. Res.*, **91**, 8411-8427, doi:10.1029/JC091iC07p08411.

Rascle, N., and F. Ardhuin, 2009: Drift and mixing under the ocean surface revisited: Stratified conditions and model-data comparisons. *J. Geophys. Res.: Oceans*, **114**, doi:10.1029/2007JC004466.

Rodríguez, E., A. Wineteer, D. Perkovic-Martin, T. Gál, B. W. Stiles, N. Niamsuwan, and R. Rodriguez Monje, 2018: Estimating ocean vector winds and currents using a Ka-band pencil-beam doppler scatterometer. *Remote Sens*., **10**, doi:10.3390/rs10040576.

Rodríguez, E., M. Bourassa, D. Chelton, J. T. Farrar, D. Long, D. Perkovic-Martin, and R. Samelson, 2019: The winds and currents mission concept. *Front. Mar. Sci.*, **6**, doi:10.3389/fmars.2019.00438.

Röhrs, J. and K. H. Christensen, 2015: Drift in the uppermost part of the ocean. *Geophys. Res. Lett.*, **42**, 10349-10356, doi:10.1002/2015GL066733.

Röhrs, J., and Coauthors, 2021: Surface currents in operational oceanography: Key applications, mechanisms, and methods. *J. Oper. Oceanogr.*, doi:10.1080/1755876X.2021.1903221.

Shinoda, T., 2005: Impact of the diurnal cycle of solar radiation on intraseasonal SST variability in the western equatorial Pacific. *J. Climate*, **18**, 2628–2636, doi:10.1175/JCLI3432.1.

Skyllingstad, E. D., and R. M. Samelson, 2020: Instability processes in simulated finite-width ocean fronts. *J. Phys. Oceanogr.*, **50**, 2781–2796, doi:10.1175/JPO-D-20-0030.1.

Smith, K. M., P. E. Hamlington, and B. Fox-Kemper, 2016: Effects of submesoscale turbulence on ocean tracers. *J. Geophys. Res.: Oceans*, **121**, 908–933, doi:10.1002/2015JC011089.

Smyth, W. D., J. N. Moum, L. Li, and S. A. Thorpe, 2013: Diurnal shear instability, the descent of the surface shear layer, and the deep cycle of equatorial turbulence. *J. Phys. Oceanogr.*, **43**, 2432– 2455, doi:10.1175/JPO-D-13-089.1.

Sun, D., and Coauthors, 2020: Diurnal cyling of submesoscale dynamics: Lagrangian implications in drifter simulations of the northern Gulf of Mexico. *J. Phys. Oceanogr.*, **50**, 1605-1623, doi:10.1175/JPO-D-19-0241.1.

Sutherland, G., L. Marié, G. Reverdin, K. H. Christensen, G. Broström, and B. Ward, 2016: Enhanced turbulence associated with the diurnal jet in the ocean surface boundary layer. *J. Phys. Oceanogr.*, **46**, 3051-3067, doi:10.1175/JPO-D-15-0172.1.

Taylor, J. R., and R. Ferrari, 2010: Buoyancy and wind-driven convection at mixed layer density fronts. *J. Phys. Oceanogr.*, **40**, 1222–1242, doi:10.1175/2010JPO4365.1.

Thomas, L. N., J. R. Taylor, E. A. D'Asaro, C. M. Lee, J. M. Klymak, and A. Shcherbina, 2016: Symmetric instability, inertial oscillations, and turbulence at the Gulf Stream front. *J. Phys. Oceanogr.*, **46**, 197–217, doi:10.1175/JPO-D-15-0008.1.

UNESCO-IOC, 2021: The United Nations Decade of Ocean Science for Sustainable Development (2021-2030) Implementation Plan. IOC Ocean Decade Series, 20, 20 pp, https://oceandecade.org/resource/109/Summary---Version-20-of-the-Ocean-Decade-Implementation-Plan.

van Sebille, and Coauthors, 2018: Lagrangian ocean analysis: Fundamentals and practices. *Ocean Model*., **121**, 49-75, doi:10.1016/j.ocemod.2017.11.008.

van Sebille, E., and Coauthors, 2020: The physical oceanography of the transport of floating marine debris. *Environ. Res. Lett.*, **15**, doi:10.1088/1748-9326/ab6d7d.

Villas Bôas, A. Band Coauthors, 2019: Integrated observations of global surface winds, currents, and waves: Requirements and challenges for the next decade. *Front. Mar. Sci.*, **6**, doi:10.3389/fmars.2019.00425.

Weller, R. A., and A. J. Plueddemann, 1996: Observations of the vertical structure of the oceanic boundary layer. *J. Geophys. Res.: Oceans*, **101**, 8789-8806, doi:10.1029/96JC00206.

Wenegrat, J. O., and M. J. McPhaden, 2015: Dynamics of the surface layer diurnal cycle in the equatorial Atlantic Ocean (0°, 23°W). *J. Geophys. Res.: Oceans*, **120**, 563–581, doi:10.1002/2014JC010504.

Wenegrat, J. O., and M. J. McPhaden, 2016a: Wind, waves, and fronts: Frictional effects in a generalized Ekman model. *J. Phys. Oceanogr.*, **46**, 371–394, doi:10.1175/JPO-D-15-0162.1.

Wenegrat, J. O., and M. J. McPhaden, 2016b: A simple analytical model of the diurnal Ekman layer. *J. Phys. Oceanogr.*, **46**, 2877–2894, doi:10.1175/JPO-D-16-0031.1.

Wenegrat, J. O., and L. N. Thomas, 2017: Ekman transport in balanced currents with curvature. *J. Phys. Oceanogr.*, **47**, 1189–1203, doi:10.1175/JPO-D-16-0239.1.

Wenegrat, J. O., L. N. Thomas, M. A. Sundermeyer, J. R. Taylor, E. A. D'Asaro, J. M. Klymak, R. K. Shearman, and C. M. Lee, 2020: Enhanced mixing across the gyre boundary at the Gulf Stream front. *Proc. Natl. Acad. Sci.*, **117**, 17607–17614, doi:10.1073/pnas.2005558117.

Whitt, D. B., and L. N. Thomas, 2015: Resonant generation and energetics of wind-forced near-inertial motions in a geostrophic flow. *J. Phys. Oceanogr*., **45**, 181–208, doi:10.1175/JPO-D-14-0168.1.

Yu, X., A. L. Ponte, S. Elipot, D. Menemenlis, E. D. Zaron, and R. Abernathey,2019: Surface kinetic energy distributions in the global oceans from a high-resolution numerical model and surface drifter observations. *Geophys. Res. Lett.*, **46**, 9757-9766, doi:10.1029/2019GL083074.

Zaron, E. D. and S. Elipot, 2021. An assessment of global ocean barotropic tide models using geodetic mission altimetry and surface drifters. *J. Phys. Oceanogr*., **51**, 63-82, doi:10.1175/JPO-D-20-0089.1.

Uncovering air-sea interaction in oceanic submesoscale frontal regions using high-resolution satellite observations

Alex Ayet[1,2,3], Nicolas Rascle[4], Bertrand Chapron[5], Fleur Couvreux[2], and Laurent Terray[3]

[1]Université Grenoble Alpes, CNRS, Inria, Grenoble INP, GIPSA-Lab, France
[2]Université de Toulouse, Météo-France, CNRS, CNRM, France
[3]Université de Toulouse, CNRS, CERFACS, CECI, France
[4]Centro de Investigación Científica y de Educación Superior de Ensenada (CICESE), México
[5]Ifremer, CNRS, IRD, Université de Bretagne Occidentale, IUEM, LOPS, France

In an enthusiastic paper 20 years ago, R. A. Brown suggested that remote sensing measurements of the ocean surface reaching resolutions of ten to hundreds of meters over 1000-km regions would open a new realm for analysis, modelling, and understanding of the atmospheric and oceanic boundary layers (Brown 2000). Twenty years later, it is too early to state that all physical processes have been extracted from those measurements. However, today, theoretical planetary boundary-layer work combined with high-resolution numerical simulations can pave the way for analysis strategies that can be systematically applied to ocean remote sensing observations. There is now hope for the serendipitous features appearing in remote sensing data to be systematically exploited. In this article we discuss what we expect to learn regarding air-sea interactions at small scales.

Active microwave synthetic aperture radars (SARs) and optical radiometers (viewing areas in and around the sunglint) are sensitive to instantaneous ocean surface roughness contrasts. Those contrasts result from variations of the steepness of short gravity and capillary waves due to their interactions with (i) an inhomogeneous near-surface wind field, (ii) nonuniform surface currents, and (iii) surface slicks accumulated by surface current convergences which suppress short waves (Alpers 1985; Munk et al. 2000; Kudryavtsev et al. 2005, 2012). The typical relaxation time and space scales of these short surface waves are smaller than 1 s and 100 m, which implies that the roughness contrast images offer a quasi-instantaneous picture of the air-sea interface.

These variations of the air-sea interface roughness are controlled by the dynamical and thermodynamical processes occurring in the marine atmospheric boundary layer (MABL, of height $O(500\text{ m})$) and in the ocean mixed layer (OML, of depth $O(50\text{ m})$), both of which are coupled over a wide range of spatio-temporal scales. In ocean frontal regions this coupling is particularly intense.

Ocean fronts can affect the MABL, inducing strong near-surface wind heterogeneities, which could then impact the OML. There is thus hope that the *imprint* of the MABL-OML coupling can be quantified through remotely sensed roughness contrasts, helping to advance the understanding of ocean-atmosphere interactions. More precisely, these high-resolution images could help better understand the transfers of heat and momentum between the ocean and atmosphere, which depend on the mixing processes (both vertical and horizontal) in the MABL and the OML, and which are essential for weather and climate models. Many spectacular manifestations of MABL and OML processes are now routinely reported in roughness images. One typical example is convection organization in the MABL, illustrated in the top panel of Figure 1, which can transition from two-dimensional rolls (with scales of 1-10 km) to three-dimensional convective cells (Atkinson and Zhang 1996). This is illustrated in Figure 2a, where Boxes 1 and 3 show typical signatures of these two- and three-dimensional MABL coherent structures respectively (as defined in Wang et al. 2020). This measurable organization can then be used to

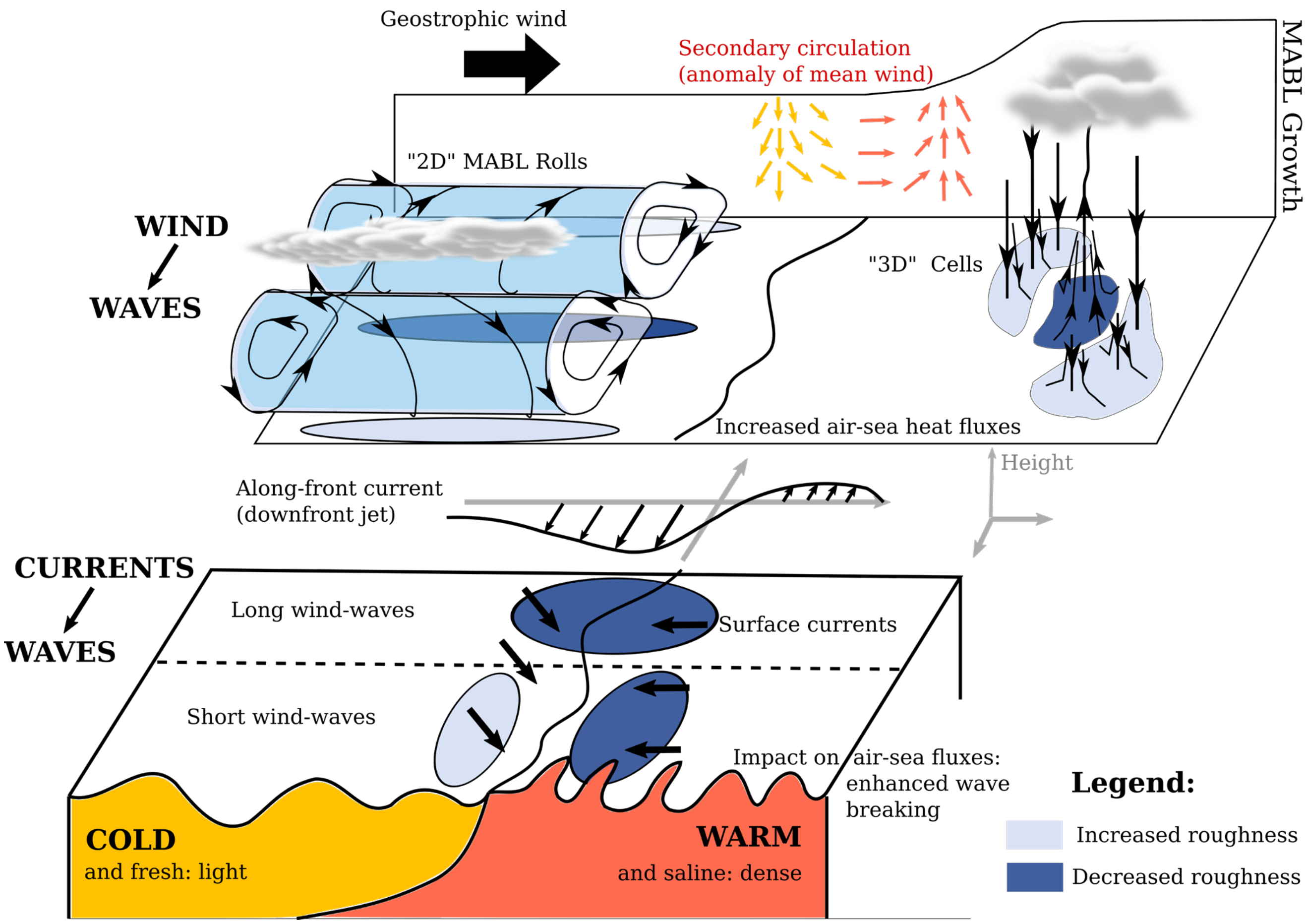

Figure 1. Sketch of the atmospheric (top panel) and oceanic (bottom panel) processes around an oceanic current front discussed in this paper. Top panel: The changes in air-sea heat fluxes and advective effects influence the MABL height and the convection organization, which can transition from MABL rolls to convective cells, thus impacting clouds and radiation. The mean wind is also affected, and secondary circulations can appear. Bottom panel: Surface currents interact with wind-waves, affecting their slope and distribution. The resulting effect depends on the wavelength of the waves. Those processes are believed to produce signatures on the sea-surface roughness, which is measurable through SARs or optical radiometers. The increased and decreased roughness areas correspond respectively to white and dark areas in Figures 2 and 4. The sketch is not to scale.

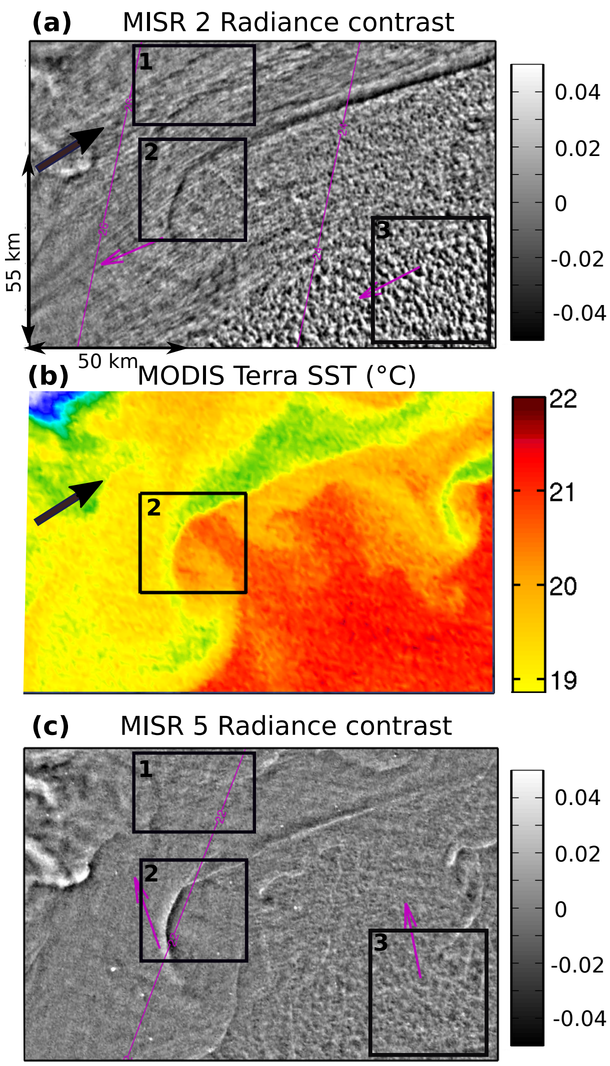

Figure 2. Quasi-simultaneous images of surface roughness and SST in the Northern Gulf of Mexico on February 11, 2016. (a) Sunglint images from Multiangle Imaging SpectroRadiometer (MISR, Chust and Sagarminaga 2007) camera #2, (b) SST from MODIS Terra, (c) Same as (a) but for MISR camera #5 viewing at a different angle. Magenta contours and arrows in (a) and (c) show respectively zenith and azimuth view angles (defined as the angles to reflect sunlight towards the satellite).

determine changes in local wind stress direction and magnitude (Beal et al. 1997; Weckwerth et al. 1997). By relying on the similarity relationships of the convective MABL, the images can also be used to infer other MABL properties such as its height (Sikora et al. 1997) and some of its turbulence statistics (Young et al. 2000). Surface roughness images also show manifestations of fine-scale current fronts at the ocean sub-mesoscale (spatial scales below 10 km). This is illustrated in the bottom panel of Figure 1 and in Figure 2a, where Box 2 shows an oceanic front, which despite being elongated over more than 10 km, is only about 50 m wide. Current gradients at this front are confirmed by in-situ buoy measurements to reach 100 f (f being the Coriolis frequency), thus largely escaping the geostrophic equilibrium (D'Asaro et al. 2018; Rascle et al 2020). Due to the large vertical velocities they induce, those fronts are hot spots for biology and drifting pollution, including plastics and seaweeds. Furthermore, current fronts are also associated with intense sea surface temperature (SST) fronts, as illustrated in the bottom panel of Figure 1, which can affect the MABL by impacting air-sea heat fluxes. The dynamics occurring at these strong frontal zones are still poorly understood, involving most probably active feedbacks between MABL, OML, and surface waves. The following section illustrates how remote sensing roughness observations could help advance our physical knowledge of those processes.

Wave-current interactions and their signature on roughness images

Around intense current fronts, at typical scales of 0.1-1 km, wave-current interactions are the dominant source of sea surface roughness contrast. For this range of scales, surface roughness directly traces the effect of current on surface waves. This effect can be inverted to estimate current fields from surface roughness observations.

Despite its apparent simplicity, this inversion involves two fairly different dynamical regimes. Very short wind-waves are in tight equilibrium with the local wind and respond quasi-locally and instantaneously when perturbed by a current gradient. On the contrary, longer wind-waves have significant propagation and response length scales before reaching back their equilibrium with the local wind (e.g., Phillips 1984). Note that here we discuss short and long wind-waves, whereas freely propagating swell

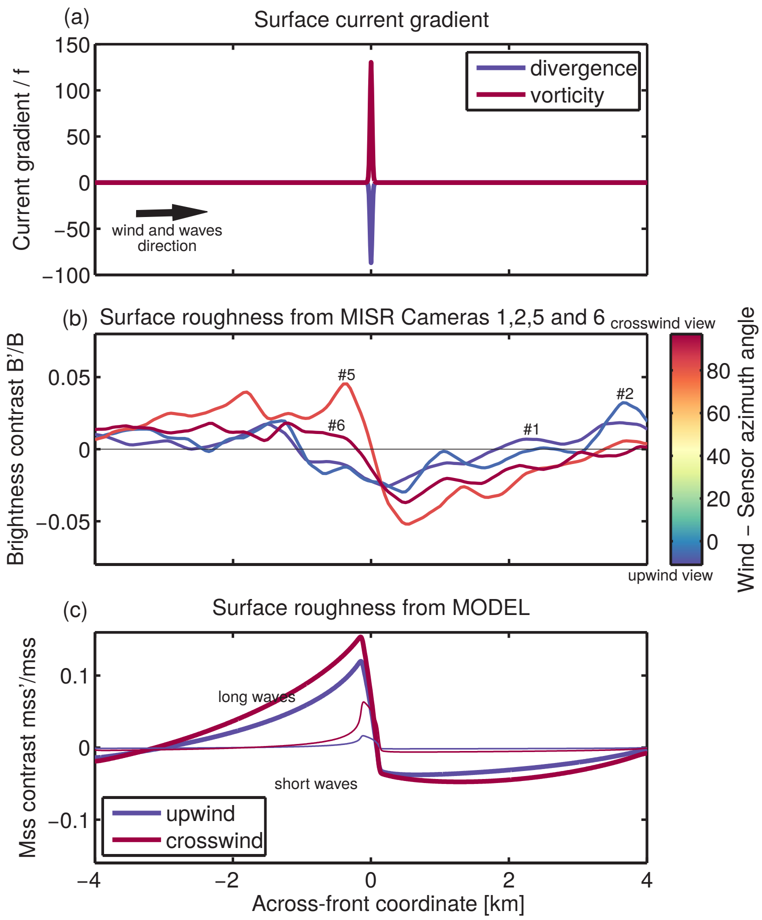

Figure 3. Transect of the current front of zone 2 of Figure 2. A sketch of the frontal currents can be found in the bottom panel of Figure 1. (a) Current gradient estimates from buoy observations at the front. (b) Surface roughness contrasts (defined here as brightness contrast) from selected MISR cameras. (c) Surface roughness contrasts (defined here as mean square slope (mss)) calculated from the wave-current interaction model of Kudryavtsev et al. (2005). Mss is divided here into upwind and crosswind components, and into long waves (k<0.6 rad/m) and short waves (k>30 rad/m) contributions.

follows yet another distinct dynamical regime (e.g. Villas Bôas et al. 2020). In addition to wavelength, wave direction relative to the current gradient is also important for refraction and/or wave steepening. Each component of the directional wave spectrum thus responds differently to the current perturbation. This is illustrated in Figure 2a and c. The two satellite roughness images were acquired quasi-simultaneously (4 minutes apart) but at different view angles (shown in magenta), which is equivalent to selecting different components of the directional wave field. It is apparent that the current front in zone 1 has two different signatures on the roughness images: a negative roughness anomaly in Figure 2a (and blue lines in Figure 3b), or a dipolar roughness anomaly in Figure 2c (and red lines in Figure 3b). Numerical simulations, using a wave model forced by the observed underlying current (Figure 3a) show, as expected, that the sharp current front induces a localized response of short waves, and a more gradual, dipolar response of long waves (Figure 3c) with a sensitivity depending on the relative direction of the waves.

These different frontal responses of the directional wave components can be exploited to retrieve information on the current field around the front. Indeed, if the frontal responses of all components were observed, then the complete current field could be retrieved. In practice, only a few components of the wave spectrum can be observed. From airborne sensors, observations of surface roughness at different view angles allow measuring enough directional components to retrieve the width, velocity shear and convergence of the current at the front (Rascle et al. 2017). From spaceborne sensors, only a few directional components can be observed (e.g. Figures 2a and c), except for the long waves that can be resolved by some sensors (e.g. Kudryavtsev et al. 2017; Ardhuin et al. 2021). The challenge is thus to develop an observing strategy to extract the current information from available surface roughness observations.

Sampling turbulence and boundary layer dynamics

Ocean frontal regions are also zones of intense interaction between SST fronts and the MABL. At the ocean mesoscale (10-100 km), these interactions have been studied through observations (Vandemark et al. 1997; Chelton et al. 2004), and they can affect both the ocean kinetic energy budget (e.g., Renault et al. 2016) and troposphere dynamics (e.g., Foussard et al. 2019).

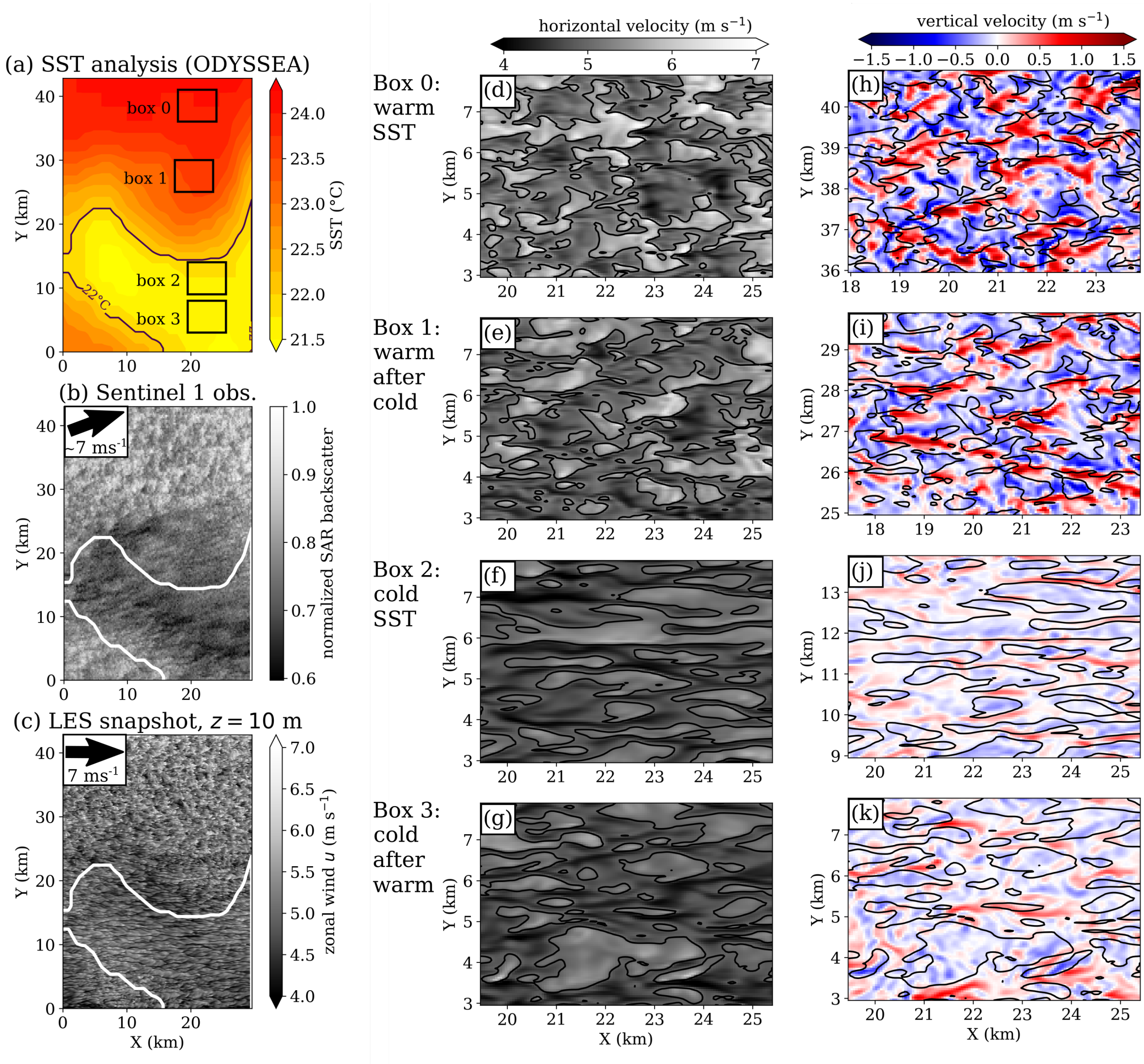

Figure 4. (a) SST analysis used to force the Large Eddy Simulation (LES) and (b) co-located surface roughness observation from Sentinel 1 (filtered at a 200m resolution). (c) Instantaneous 10-m zonal wind from the LES after reaching a quasi-equilibrium state. In (b) and (c) the black arrow indicates the observed wind direction/speed [in (b)], and the geostrophic direction/speed used to force the LES [in (c)]. Instantaneous quantities from the atmospheric LES in each of the boxes of Figure 4 (a). [(d)-(g)] Instantaneous zonal wind speed at 10-m height. Here and in [(h)-(k)], black contours indicate regions where the 10-m zonal wind exceeds its horizontal average over the box by 5%. [(h)-(k)] Instantaneous vertical wind speed at the middle of the boundary layer. Note that, in the LES, moisture, clouds, precipitation, and radiative fluxes are not considered.

However, little is known at the small scales discussed in the previous section (below 10 km), where nonlinear MABL dynamics are expected to become dominant (e.g., Sullivan et al. 2020). A case study in the Agulhas current, for which a submesoscale SST front was observed, illustrates how roughness images can help address this problem (Figure 4a, about 1°C over 10 km). The co-located roughness (SAR) image (Figure 4b) exhibits different textures, which are reminiscent of the convection-related signatures discussed in Figure 2a and the introduction.

The MABL physics behind these fine-scale structures is investigated using a high-resolution simulation (Large Eddy Simulation, LES, using the Meso-NH model, Lac et al. 2018) with horizontal resolution of 50 m and a vertical resolution varying from 2 m close to the surface to 20 m at 2 km height (the top of our domain). The simulation is forced by a homogeneous wind, and by the observed SST (Figure 4a) as a fixed-in-time bottom boundary condition, which impacts surface heat and momentum fluxes. Hence, all horizontal heterogeneities observed in the simulation can be attributed to the influence of the heterogeneous SST field on the MABL.

Figure 4c shows a snapshot of the simulated 10-m zonal wind speed over the simulation domain. It is strongly heterogeneous, with different textures comparable to those of Figure 4b, with however several differences: (i) the scale of the structures is larger in the SAR observation than in the LES; and (ii) the orientation of the structures is not the same in the LES (aligned in the zonal direction) than in the SAR image (where there is a meridional tilt). This second difference (ii) is an effect of the idealized LES set-up, for which a purely zonal wind has been imposed to ensure periodic boundary conditions (instead of the slightly tilted observed wind, shown in Figure 4b). As for difference (i), it could be attributed to a filtering effect of wind-waves. Due to their adjustment timescale, remotely-sensed wind-waves could end up being sensitive only to large enough atmospheric scales. Nonetheless, what the simulation shows is that the presence of different textures in the SAR observation can be attributed to the effect of the SST on the MABL.

A closer look to the different simulated textures in Figure 4d-g shows that, on the cold side of the domain (Figure 4f), the zonal wind structures are more elongated than on its warm side (Figure 4d and 4e). Those zones of strong zonal surface wind are well correlated with the downward vertical velocities at the middle of the MABL (compare black contours and red zones in Figures 4h-k). This shows that these near surface textures can be related to different organizations of convection and to coherent structures in the MABL (which transport high-momentum fluid downward, see the top panel of Figure 1): three-dimensional cells for a warmer SST (Boxes 0 and 1) and two-dimensional rolls for a colder SST (Box 2).

The case of Box 3 is however interesting. Even though the SST is similar to Box 2 in this area, the organization of convection does not have the same characteristic scales as Box 2. It is a transition regime between the three-dimensional cells of Boxes 0 and 1 and the rolls of Box 2. The MABL height of Box 3 (450 m) is also larger than the one in Box 2 (350 m, not shown). This shows that for these sharp frontal configurations, SST is not the only driver of MABL dynamics, and that advective effects could also play a role (see e.g., Sullivan et al. 2020). These changes are also associated with secondary circulations (see the sketch in the top panel of Figure 1), of particular interest to modelers as they relate to large-scale divergence (see e.g., the analytical formulas in Ayet and Redelsperger 2019) and affects the free troposphere (e.g., Feliks et al. 2004; Foussard et al. 2019).

Conclusion and outlook

This paper illustrates that high-resolution remote sensing images of ocean surface roughness, combined with theoretical and high-resolution numerical models, can provide physical insights into the air-sea interactions happening in intense ocean frontal regions. In particular: (i) local variations in surface roughness (due to currents and winds) can be detected; (ii) strong near-surface currents can be quantified; and (iii) changes in atmospheric convective organization and secondary circulations can be quantified and attributed to SST-MABL interactions. For (ii) and (iii), the paper highlights the limitations of the methodologies used to extract information from the images, which require a deeper understanding of wind-wave-current interactions (see also Villas Bôas and Pizzo, this issue).

A lot still remains to be done in order to understand the coupled MABL-OBL system at fine scales. While some hints about the effect of SST gradients on the MABL exist, the effect of the strong current fronts on the MABL, through changes in surface roughness, is still not assessed. Those non-local changes affect whitecap coverage and should thus change ocean-atmosphere fluxes of momentum, heat, and gas. Wave-current coupling and ocean-atmosphere coupling thus become largely entangled. The changes in MABL convection organization also have important implications: (i) they likely affect the cloud organization and radiative properties of the MABL (Villefranque 2019); and (ii) they could affect the OML and its mixing properties. Point (i) highlights the need to use multimodal sensors that are capable of measuring cloud properties, roughness, currents, and SST almost simultaneously. Missions including multimodal sensors include the upcoming SWOT (Morrow et al. 2019), foreseen Harmony (ESA 2020) and proposed Seastar (Gommenginger et al. 2019) mission concepts. Point (ii) still remains to be assessed, and could require (a) understanding of how higher-order quantities of the current field, like secondary circulations and Langmuir circulations, can be extracted from roughness images and (b) using high-resolution coupled numerical simulations, which are still not at hand.

Nonetheless, a new age in the use of near-surface ocean observations and high-resolution numerical simulations is gradually emerging. Thinking about climate models, roughness images provide data-rich statistics about MABL-OML fine-scale coupling processes that can be used to constrain the development of new parameterizations and included in model evaluation metrics. We believe that properly using this information requires a combination of both observations, simulations and theory, which means developing dedicated, physic-informed statistical methods able to extract physical laws from multimodal remote sensing data.

Acknowledgments

AA thanks Fabrice Collard for providing the satellite data for the simulation as well as for the interesting discussions. AA was funded by a CNES post-doctoral grant. We acknowledge the use of The Atmospheric Science Data Center (ASDC) at NASA Langley Research Center for the MISR data.

References

Alpers, W., 1985: Theory of radar imaging of internal waves. *Nature*, **314**, 245-247, doi:10.1038/314245a0.

Ardhuin, F., M. Alday, and M. Yurovskaya, 2021: Total surface current vector and shear from a sequence of satellite images: Effect of waves in opposite directions. *J. Geophys. Res.: Oceans*, **126**, doi:10.1029/2021JC017342.

Atkinson, B. W., and J. Wu Zhang, 1996: Mesoscale shallow convection in the atmosphere. *Rev. Geophys.*, **34**, 403-431, doi:10.1029/96RG02623.

Ayet, A., and J.-L. Redelsperger, 2019: An analytical study of the atmospheric boundary-layer flow and divergence over an SST front. *Quart. J. Roy. Meteor. Soc.*, **145**, 2549-2567, doi:10.1002/qj.3578.

Beal, R. C., V. N. Kudryavtsev, D. R. Thompson, S. A. Grodsky, D. G. Tilley, V. A. Dulov, and H. C. Graber, 1997: The influence of the marine atmospheric boundary layer on ERS 1 synthetic aperture radar imagery of the Gulf Stream. *J. Geophys. Res.: Oceans*, **102**, 5799-5814, doi:10.1029/96JC03109.

Brown, R. A., 2000: Serendipity in the use of satellite scatterometer, SAR, and other sensor data. *Johns Hopkins APL Tech. Dig.*, **21**, 21-26.

Chelton, D. B., M. G. Schlax, M. H. Freilich, and R. F. Milliff, 2004: Satellite measurements reveal persistent small-scale features in ocean winds. *Science,* **303**, 978–983, doi:10.1126/science.1091901.

Chust, G., and Y. Sagarminaga, 2007: The multi-angle view of MISR detects oil slicks under sun glitter conditions. *Remote Sens. Environ.*, **107**, 232-239, doi:10.1016/j.rse.2006.09.024.

D'Asaro, E. A., and Coauthors, 2018: Correction for D'Asaro et al., Ocean convergence and the dispersion of flotsam. *Proc. Natl. Acad. Sci.*, **115**, doi:10.1073/pnas.1802701115.

ESA, 2020: Report for assessment: Earth Explorer 10 Candidate Mission Harmony. 133 pp, https://esamultimedia.esa.int/docs/EarthObservation/EE10_Harmony_Report-for-Assessment-v1.0_13Nov2020.pdf.

Feliks, Y., M. Ghil, and E. Simonnet, 2004: Low-frequency variability in the midlatitude atmosphere induced by an oceanic thermal front. *J. Atmos. Sci.*, **61**, 961-981, doi:10.1175/1520-0469(2004)061<0961:LVITMA>2.0.CO;2.

Foussard, A., G. Lapeyre, and R. Plougonven, 2019: Storm track response to oceanic eddies in idealized atmospheric simulations. *J. Climate*, **32**, 445-463, doi:10.1175/JCLI-D-18-0415.1.

Gommenginger, C., and Coauthors, 2019: SEASTAR: A mission to study ocean submesoscale dynamics and small-scale atmosphere-ocean processes in coastal, shelf and polar seas. *Front Mar. Sci.*, **6**, doi:10.3389/fmars.2019.00457.

Kudryavtsev, V., D. Akimov, J. Johannessen, and B. Chapron, 2005: On radar imaging of current features: 1. Model and comparison with observations. *J. Geophys. Res.: Oceans*, **110**, doi:10.1029/2004JC002505.

Kudryavtsev, V., A. Myasoedov, B. Chapron, J. A. Johannessen, and F. Collard, 2012: Imaging mesoscale upper ocean dynamics using synthetic aperture radar and optical data. *J. Geophys. Res.*, **117**, doi:10.1029/2011JC007492.

Kudryavtsev, V., M. Yurovskaya, B. Chapron, F. Collard, and C. Donlon, 2017: Sun glitter imagery of surface waves. Part 2: Waves transformation on ocean currents. *J. Geophys. Res.: Oceans*, **122**, 1384–1399, doi:10.1002/2016JC012426.

Lac, C., and Coauthors, 2018: Overview of the Meso-NH model version 5.4 and its applications. Geosci. Model Dev., 11, 1929-1969, doi:10.5194/gmd-11-1929-2018.

Morrow, R., and Coauthors, 2019: Global observations of fine-scale ocean surface topography with the Surface Water and Ocean Topography (SWOT) mission. *Front. Mar. Sci.*, **6**, doi:10.3389/fmars.2019.00232.

Munk, W., L. Armi, K. Fischer, and F. Zachariasen, 2000: Spirals on the sea. *Proc. Roy. Soc. London, Ser. A*, **456**, 1217-1280, doi:10.1098/rspa.2000.0560.

Phillips, O. M., 1984: On the response of short ocean wave components at a fixed wavenumber to ocean current variations. *J. Phys. Oceanogr.*, **14**, 1425-1433, doi:10.1175/1520-0485(1984)014<1425:OTROSO>2.0.CO;2.

Rascle, N., J. Molemaker, L. Marié, F. Nouguier, B. Chapron, B. Lund, and A. Mouche, 2017: Intense deformation field at oceanic front inferred from directional sea surface roughness observations. *Geophys. Res. Lett.*, **44**, 5599– 5608, doi:10.1002/2017GL073473.

Rascle, N., and Coauthors, 2020: Monitoring intense oceanic fronts using sea surface roughness: Satellite, airplane, and in situ comparison. *J. Geophys. Res.: Oceans*, **125**, doi:10.1029/2019JC015704.

Renault, L., M. J. Molemaker, J. C. McWilliams, A. F. Shchepetkin, F. Lemarié, D. Chelton, S. Illig, and A. Hall, 2016: Modulation of wind work by oceanic current interaction with the atmosphere. *J. Phys. Oceanogr.*, **46**, 1685-1704, doi:10.1175/JPO-D-15-0232.1.

Sikora, T. D., G. S. Young, H. N. Shirer, and R. D. Chapman, 1997: Estimating convective atmospheric boundary layer depth from microwave radar imagery of the sea surface. *J. Appl. Meteor.*, **36**, 833-845, doi:10.1175/1520-0450(1997)036<0833:ECABLD>2.0.CO;2.

Sullivan, P. P., J. C. McWilliams, J. C. Weil, E. G. Patton, and H. J. Fernando, 2020: Marine boundary layers above heterogeneous SST: Across-front winds. *J. Atmos. Sci.*, **77**, 4251-4275, doi:10.1175/JAS-D-20-0062.1.

Vandemark, D., J. B. Edson, and B. Chapron, 1997: Altimeter estimation of sea surface wind stress for light to moderate winds. *J. Atmos. Oceanic Technol.*, **14**, 716-722, doi:10.1175/1520-0426(1997)014<0716:AEOSSW>2.0.CO;2.

Villas Bôas, A. B., B. D. Cornuelle, M. R. Mazloff, S. T. Gille, and F. Ardhuin, 2020: Wave–current interactions at meso- and submesoscales: Insights from idealized numerical simulations. *J. Phys. Oceanogr.*, **50**, 3483-3500, doi:10.1175/JPO-D-20-0151.1.

Villefranque, N., 2019: Les effets radiatifs 3D des nuages de couche limite: De leur simulation explicite à leur paramétrisation. PhD dissertation, Université Paul Sabatier - Toulouse III, 274 pp, https://tel.archives-ouvertes.fr/tel-02628562/document.

Wang, C., D. Vandemark, A. Mouche, B. Chapron, H. Li, and R. C. Foster, 2020: An assessment of marine atmospheric boundary layer roll detection using Sentinel-1 SAR data. *Remote Sens. Environ.*, **250**, doi:10.1016/j.rse.2020.112031.

Weckwerth, T. M., J. W. Wilson, R. M. Wakimoto, and N. A. Crook, 1997: Horizontal convective rolls: Determining the environmental conditions supporting their existence and characteristics. *Mon. Wea. Rev.*, **125**, 505-526, doi:10.1175/1520-0493(1997)125<0505:HCRDTE>2.0.CO;2.

Young, G. S., T. D. Sikora, and N. S. Winstead, 2000: Inferring marine atmospheric boundary layer properties from spectral characteristics of satellite-borne SAR imagery. *Mon. Wea. Rev.*, **128**, 1506-1520, doi:10.1175/1520-0493(2000)128<1506:IMABLP>2.0.CO;2.

The geometry, kinematics, and dynamics of the two-way coupling between wind, waves, and currents

Ana B. Villas Bôas[1,2] and Nick Pizzo[3]

[1]California Institute of Technology
[2]Colorado School of Mines
[3]University of California San Diego, Scripps Institution of Oceanography

Fundamental and sometimes spectacular exchanges of mass, momentum, heat, and energy occur where the ocean and atmosphere meet. This region, known as the air-sea boundary layer, is of crucial importance for Earth's weather and climate. There, wind, waves, and currents interact in complicated and striking ways. Below is a review of these interactions through the lens of their geometry, kinematics, and dynamics, including an overview of what the community knows, admittedly from a wave-centric point of view, highlights of some important open questions, and a recommendation for future observational campaigns (for more comprehensive reviews see Melville 1996; Sullivan and McWilliams 2010; D'Asaro 2014).

Present observational capabilities

Although the oceanographic and climate communities now recognize that processes happening at the air-sea boundary layer are intrinsically coupled, observational, theoretical, and modeling efforts have traditionally focused on each of these processes independently. There is much that remains unknown about the contribution of the three-way coupling between winds, currents, and waves to the climate system (Villas Bôas et al. 2019). A schematic of this coupling is shown in Figure 1. These interactions are intrinsically multiscale, ranging from millimeters for spray and capillary waves to 100s of kilometers for mesoscale currents, which poses a challenge for observations.

At global scales, spaceborne scatterometers, altimeters, and radiometers have for decades provided a large-scale view of surface winds, sea surface height, and sea surface temperature. More recently, satellites using synthetic aperture radar (SAR) technology have not only increased the resolution of sea surface height measurements but have also made it possible to image the sea surface roughness and capture the signature of boundary-layer processes such as surface waves, submesoscale features, and wind streaks (Kudryavtsev et al. 2017; Wang et al. 2019; Yurovskaya et al. 2019). The launch of the Chinese-French Oceanography Satellite (CFOSAT) in 2018 marked the beginning of a new era for observations of air-sea interactions (Hauser et al. 2019), where for the first time it is possible to measure directional wave information and surface winds simultaneously at global scales. Nonetheless, there are still fundamental gaps in the present observing system that limit the understanding of boundary-layer processes. In particular,

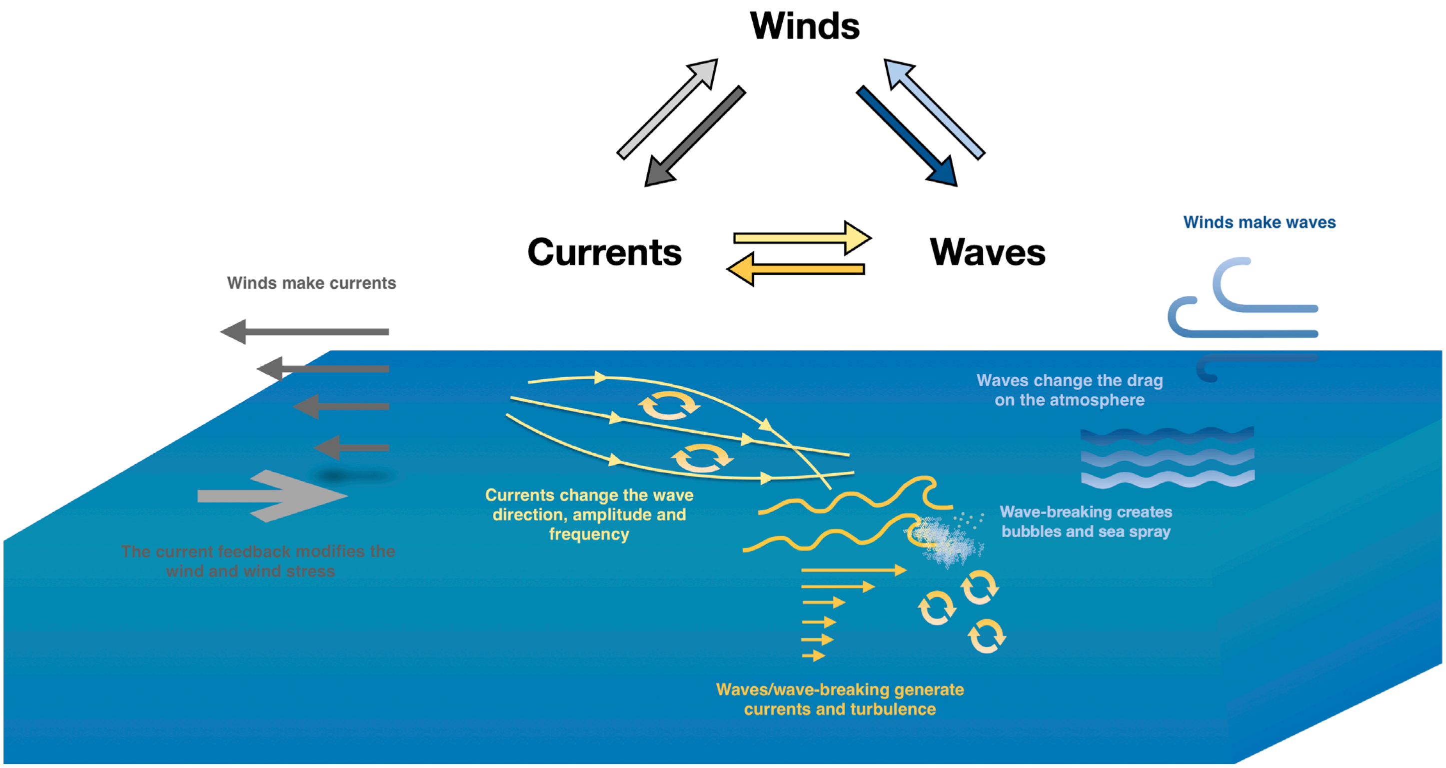

Figure 1. A schematic of the full two-way coupling between wind, waves, and currents considered in this paper. Examples of these interactions are indicated, with the color corresponding to the direction of interaction indicated by the prism

these phenomena are strongly coupled, so there is a need for simultaneous co-located observations of winds, currents, waves, temperature, and humidity over a broad range of scales and environmental conditions in order to test existing theories and refine (or redefine altogether) present model parameterizations.

Sea-surface geometry

One of the first things people notice when going out to sea, particularly if they have a sensitive stomach, is that the ocean surface is not flat. This has important implications for fluxes between the air and sea, which are by definition a function of the surface area separating the two fluids. For example, the transfer of carbon dioxide (CO_2) and other gases between the atmosphere and ocean is greatly increased by the surface area of spray and bubbles created by wave breaking (Veron 2015; Deike et al. 2017b). Additionally, the geometry of the waves changes how momentum is fluxed from the wind to the water. That is, while it is somewhat intuitive that winds affect surface waves, waves can also affect the wind stress by modulating the sea surface roughness (Edson et al. 2013).

Waves are strongly affected by currents, which can modulate their frequency, direction, and amplitude (Phillips 1977). Thus, wave-current interactions play a fundamental role in the geometry of the sea surface. Although surface waves are often regarded as noise in most remote sensing measurements, the signature of currents on waves encodes important information that can be used to infer properties of the underlying current field. This is an idea that has been around for decades (e.g., Stewart and Joy 1974; Phillips 1984). However, despite the maturity of some of these theoretical ideas, there is currently no systematic way of using wave measurements to infer information about the currents. This inverse problem remains very much at the forefront of the field.

As new remote sensing technologies to measure ocean surface emerge, there is an increasing need to better understand and characterize the impact of waves on radar and lidar measurements. Jules Charney once remarked that the ocean surface does not really "look the same upside-down," which is due to the fact that ocean waves have pointier crests and flatter troughs (Laughton et al. 2010). This implies that for nadir altimeters more radar power is reflected back from the trough of waves than the crests, giving rise to the so-called electromagnetic (EM) bias (Fu and Glazman 1991; Melville et al. 1991). Theoretical models of this bias predict a linear relationship between the EM bias and the significant wave height. However, other characteristics of the sea state, such as the degree of wave development (wave age), the wind speed, and the direction of the waves, also contribute to the EM bias (Melville et al. 2004). Thus, as satellite altimeters evolve towards resolving finer spatial scales, precise knowledge of the wave field will be key to understanding how surface waves contribute to the error budget of sea surface height measurements.

In the context of the upcoming Surface Water and Ocean Topography mission (SWOT, Morrow et al. 2019), other errors related to the sea surface geometry will also be important. SWOT will be equipped with a wide swath SAR altimeter that will measure the sea surface height at an order of magnitude higher spatial resolution than present altimeters. Because the footprint of SWOT will be comparable to the wavelength of surface waves, non-linear effects can result from multiple points at the sea surface that are within the same radar range mapping into a single point, a phenomenon known as the surfboard effect (Peral et al. 2015).

Another aspect of surface waves that deserves particular attention is that the wave field is highly directional and anisotropic (Longuet-Higgins 1962; Lenain and Melville 2017; Romero 2019). Measurements from narrow-swath instruments effectively take a 1D slice through the 2D wave field which can alias wave energy onto lower wavenumbers and frequencies. Recently, Yu et al. (2020) investigated this effect on sea surface height measurements from the Ice, Cloud and land Elevation Satellite (ICESat-2) and emphasized the importance of directional wave information to interpret the sea surface height signal at scales shorter than the mesoscale. Many of the implications that waves have for remote sensing depend on details of the sea surface geometry that are more complex than what is captured by bulk low order parameters such as significant wave height.

What we do not know. Physically, there is still much to learn about the volume of air entrained due to wave breaking (see, for example, Brumer et al. 2017) and how this modulates gas transfer at the ocean surface. Additionally, modern research on wave generation by wind has moved away from drag law parameterizations and has instead focused on elucidating particular mechanisms of wave generation (Janssen 2004; Grare et al. 2013; Buckley and Veron 2016). However, there is still considerable uncertainty for momentum and gas transfer at the ocean surface, while the two-way coupling between wind and waves remains an open question. More practically, it remains unclear how the sea state (beyond the bulk parameters), and in particular wave breaking, affects the free surface geometry and how this modifies measurements from remote sensing instruments, such as radar and lidar.

Kinematics

Wave effects on currents. The particle trajectories of irrotational surface waves are not closed, but slightly open, leading to a net transport in the direction of wave propagation known as Stokes drift. This, together with wave breaking (Deike et al. 2017a; Pizzo et al. 2019), forms the wave-induced mass transport at the ocean surface. The current induced by waves can often exceed Ekman currents and is an important component of the total surface current velocity, which is essential for transporting jetsam, flotsam, plastics, pollutants, algae, and ice (van Sebille et al. 2020).

Current effects on waves. Surface waves not only generate currents but also interact with existing currents.

For slowly-varying currents, the kinematics of this interaction are well-known and can be described by geometrical optics. Perhaps the most intuitive effect that currents have on waves is through their Doppler shift in the wave dispersion relationship. In the presence of currents, the wave energy is no longer conserved due to the exchanges of energy between currents and waves. Instead, the wave action, the ratio between the wave energy and the intrinsic frequency of the waves, is conserved. Waves propagating over an opposing current will experience an increase in frequency, which leads to a corresponding increase in wave energy in order for action to be conserved (the opposite is true for co-flowing current and waves). This modulation of the wave frequency and wavenumber by currents shows up in radar and optical imagery as a deviation from the linear dispersion relationship, and it can be used to estimate current magnitude and direction. This technique has been applied to field and airborne measurements as well as sparse images from optical satellites (e.g., Sentinel-2), but the technology necessary to measure surface currents globally has yet to be implemented. A step in this direction was taken with the conceptualization of the ocean Surface TRansport, kinetic Energy, Air-sea fluxes and Mixing (STREAM) mission. However, there are no current plans to fly such a mission.

Figure 2. Photograph taken from an airplane off the coast of California showing an area of enhanced wave breaking in the upper right corner due to wave-current interaction. The horizontal length scale of the image is on the order of a kilometer. Photograph courtesy of Nick Statom, Scripps Institution of Oceanography.

In the same way that gradients in the water depth cause waves approaching the shore to change direction (refract), horizontal current gradients can change the wavenumber and direction of waves. These changes in wave direction ultimately result in convergences and divergences of wave action that can lead to spatial gradients in wave height, slope, and breaking statistics (Figure 2). Descriptions of the relationship between vertical vorticity and the curvature of individual ocean wave rays date back to Kenyon (1971). Yet, it is only recently that studies based on numerical modeling and remote sensing observations have shown that the spatial variability of the surface wave field at mesoscales is dominated by the spatial variability of currents. More specifically, theoretical (e.g., Villas Bôas and Young 2020), numerical (e.g., Romero et al. 2020; Villas Bôas et al. 2020; Marechal and Ardhuin 2021), and observational (Quilfen et al. 2018; Quilfen and Chapron 2019) studies focusing on swell-type waves have found that surface wave properties are most sensitive to current vorticity and that refraction is the main mechanism controlling the spatial variability of wave heights. Meanwhile, models suggest that short wind-waves (O(1) m), which are the main contributor to the mean square slope and sea surface roughness, may be more influenced by current divergence and strain (Rascle et al. 2014, 2016; Lenain and Pizzo 2021). Despite this compelling evidence for the strong effects of currents on waves across various scales, operational wave models are still routinely run without current forcing.

Current effects on winds. Surface currents modify work done by the winds on the ocean, as it is the relative velocity of the wind that enters the wind-work formulation, not its absolute value. The wind work is key for the kinetic energy (KE) budget of the ocean, having implications for near-inertial oscillations, mesoscale eddies, and the mean ocean circulation. Results based on coupled numerical models and remote sensing observations (Renault et al. 2017; Julien et al. 2020) have shown that this current feedback represents a sink of eddy KE (EKE) from the ocean to the atmosphere, acting as an "eddy-killer," and there are suggestions that the two-way coupling between ocean and atmosphere affects this EKE sink (Renault et al. 2016; Flexas et al. 2019). These results underline the importance of considering the relative wind in numerical models, including in wave models (Rapizo et al. 2018), and show a need for simultaneous measurements of ocean vector winds and total surface current in order to better constrain the ocean KE budget. Although we have decades of global ocean surface vector wind measurements, the currents used to compute the wind work are often geostrophic currents estimated from satellite altimetry, which cannot be estimated near the equator, are fairly limited in spatial resolution (100s of kilometers), and only account for part of the total surface current.

What we do not know. An important practical and physical problem for understanding the kinematics of these interactions involves the current shear profile. Information about the current's vertical structure would, for example, allow one to map surface measurements of the current to its behavior at depth. There is indication that wave measurements help better understand this inverse problem, but considerable practical barriers exist, including quantifying the uncertainty in the inversion process (Campana et al. 2017) and the interesting question of whether or not critical layers (i.e., areas of the flow with speeds equal to the phase velocity of a surface gravity wave) exist in the water for very short waves. Additionally, there are theoretical features of wave-current interaction that are only now being constrained, including their two-way coupling (Phillips 2002; McWilliams et al. 2004; McWilliams 2016; Suzuki 2019; Pizzo and Salmon 2021). In order to validate these problems, concurrent measurements of the wind, waves, and currents, and in particular, the current depth profiles, must be conducted – a primary aim of the NASA S-MODE Earth Venture Suborbital-3 (Farrar et al. 2020). There is excitement that a fleet of uncrewed platforms, together with state-of-the-art in-situ and airborne measurements of surface wind, currents, and waves, might be a first step in making progress on this important problem.

Dynamics

Heat is a form of energy and, together with CO_2, is among the most relevant variables to track in our warming planet. The ocean acts as a massive solar panel, absorbing around 90% of the heat imbalance in the Earth system. The ocean also takes up ~30% of the CO2 that is released in the atmosphere, through both the physical and the biological carbon pump (Sarmiento and Gruber 2006). The dynamical budget of heat and carbon is strongly mediated by fluxes that happen at the air-sea boundary layer and are controlled by processes that mix these properties from the upper ocean down to the ocean interior. Thus, processes that contribute to vertical transport and mixing are of crucial importance for Earth's climate.

Most of the energy that is transmitted to the wave field by the wind is locally converted into turbulent mixing and heat and sound generation, predominantly accomplished by wave breaking (Melville 1996). Some of this energy generates the so-called "wind-driven" currents. Wave breaking directly affects dissipation in the upper layer of the ocean (D'Asaro 2014). This is parameterized by an eddy viscosity, which implies that waves could affect larger-scale processes like Ekman flow. The direct effects of surface waves on larger-scale flow are still an open question, but there is theoretical (McWilliams and Restrepo 1999; Shrira and Almelah 2020) and numerical (Lewis and Belcher 2004; Sullivan et al. 2007; Sullivan and McWilliams 2010) evidence that surface waves can affect currents at much larger scale than the waves themselves.

Wave breaking also introduces vorticity into the ocean. This vorticity then interacts with the Stokes drift, generating Langmuir circulation and Langmuir turbulence, which mixes the upper ocean and deepens the mixed layer. Note, the vertical shear of the Stokes drift shows up in the turbulent kinetic energy budget, not the Stokes drift itself. This upper-ocean mixing sets the temperature difference between the air and sea – a crucial value for coupled air-sea models. However, numerical models represent unresolved processes that control vertical mixing through parametrization schemes that often do not explicitly take into account the effects of surface waves. Observed biases in the mixed-layer depth in a number of climate models (Verdy et al. 2014; Li et al. 2016) suggest that there could be processes relevant for turbulent mixing that have been ignored in most parameterizations of the mixed layer. Despite the obvious importance of these processes, the details of these phenomena remain poorly understood, as discussed below.

Finally, the characteristics of winds, waves, and currents vary strongly geographically and seasonally. Local changes in winds modulate the wave field, which may, in turn, affect mixed layer depths through enhanced mixing due to the Langmuir turbulence mentioned above. This can, for example, lead to deeper mixed layers and stronger submesoscale activity, whereas in the absence of wave-induced turbulence, shallower mixed-layers with strong stratification at their base may encourage internal wave generation and inhibit the vertical motions associated with (horizontally divergent) submesoscale currents. Hence, to better understand processes such as internal waves and submesoscale fronts, we must better constrain the impact of wave-driven mixing to upper ocean dynamics.

What we do not know. The so-called Craik-Leibovich (CL) equations governing Langmuir circulations/turbulence have not been validated against laboratory/field data in a meaningful way, leaving their applicability uncertain. In general, they are found to reduce the bias between modeled mixed-layer depths and observations, but the detailed comparisons between model output and observations from a controlled environment remain scarce. This is because there are only a very small number of observations of mixed layer deepening on the space and time scales necessary to resolve the genesis and evolution of the process (Smith 1992; Grare et al. 2021). Additionally, these limited observations exist for just a few environmental conditions. This represents a major gap in our knowledge, particularly as the CL equations are being more commonly employed in coupled air-sea boundary layer models of weather and climate.

A vision for future observations

Although the study of wind, waves, and currents is mature, there are still fundamental open questions regarding the two-way coupling between these complex phenomena. Researchers are optimistic that progress will be made to tackle these questions. First and foremost, it is currently the golden age of observational and computational oceanography. Existing, soon to be launched, and future satellite missions will provide unprecedented coverage of global winds, waves, and currents, despite the caveats discussed above. The *Earth system response to air-sea interactions* has been identified as a priority in the National Academy of Sciences Decadal Survey for Earth Science and Applications from Space. In response to that, mission concepts for satellites targeting the air-sea boundary layer have been developed and have the potential to be selected by NASA in the upcoming decade (e.g., Rodriguez et al. 2019; Gentemann et al. 2020). Crucially, the geometry, kinematics, and dynamics of wind, waves, and currents need to be *simultaneously* measured across a broad range of scales and environmental conditions for progress to be made.

Interactions between wind, waves, and currents play a major role in the exchange of momentum, heat, energy, and gases between the ocean and the atmosphere. To push the envelope of weather forecasting, climate predictions and projections, and designing of mitigation and adaptation strategies in response to climate change, requires understanding the physical processes that control air-sea exchanges in order to properly parametrize them in numerical models. Dedicated process studies in the fashion of the upcoming Submesocale Ocean Dynamics Experiment (S-MODE) will be pivotal to fostering the development of coupled atmosphere-wave-ocean models and to better constrain the parameter space for validation and development of new model parametrizations. The wealth of data that will become available in the upcoming decades will also provide a unique opportunity to explore physically constrained, data-driven solutions that can help to disentangle some of the complexities of these boundary layer processes. At the oceanographic and atmospheric community level, there is a need to entrain theoretical (Emanuel 2020), numerical, laboratory, and field scientists into the task. Central to this collaborative approach will be open-science based around open-source software, reproducibility, data availability, and transparent discussions of theoretical, numerical, and observational limitations (Wilkinson et al. 2016). Significant progress in Earth sciences will come from a cultural change that pushes the community in this direction. Finally, there is a need for a more diverse community in the Earth sciences field (Goldberg 2019). Hopefully current and future endeavors to understand wind, waves, and currents will place a high priority on building a broader community that reflects the population of the United States and the world to tackle these problems of global importance.

Acknowledgments

Both authors made equal contributions to this manuscript. We thank Sarah Gille, Matt Mazloff, Aneesh Subramanian, Andy Thompson for their comments on this manuscript. ABVB is supported by NASA award 80NSSC19K1004. NP Is supported by NASA award 80NSSC19K1688 and grants from the Physical Oceanography programs at the Office of Naval Research (N00014-17-1-2171, N00014-14-1-0710, N00014-17-1-3005, and N00014-19-1-263).

References

Brumer, S. E., C. J. Zappa, B. W. Blomquist, C. W. Fairall, A. Cifuentes-Lorenzen, J. Edson, I. M. Brooks, and B. J. Huebert, 2017: Wave-related Reynolds number parameterizations of CO2 and DMS transfer velocities. *Geophys. Res. Lett.*, **44**, 9865-9875, doi:10.1002/2017GL074979.

Buckley, M. P., and F. Veron, 2016: Structure of the airflow above surface waves. *J. Phys. Oceanogr.*, **46**, 1377-1397, doi:10.1175/JPO-D-15-0135.1.

Campana, J., E. J. Terrill, and T. de Paolo, 2017: A new inversion method to obtain upper-ocean current-depth profiles using X-band observations of deep-water waves. *J. Atmos. Oceanic Technol*., **34**, 957-970, doi:10.1175/JTECH-D-16-0120.1.

D'Asaro, E. A., 2014: Turbulence in the upper-ocean mixed layer. *Annu. Rev. Mar. Sci*., **6**, 101-115, doi:10.1146/annurev-marine-010213-135138.

Deike, L., L. Lenain, and W. K. Melville, 2017a: Air entrainment by breaking waves. *Geophys. Res. Lett.*, **44**, 3779-3787, doi:10.1002/2017GL072883.

Deike, L., N. Pizzo, and W. K. Melville, 2017: Lagrangian transport by breaking surface waves. *J. Fluid Mech*., **829**, 364-391, doi:10.1017/jfm.2017.548.

Deike, L., L. Lenain, and W. K. Melville, 2017b: Air entrainment by breaking waves. *Geophys. Res. Lett.*, **44**, 3779-3787, doi:10.1002/2017GL072883.

Edson, J. B., and Coauthors, 2013: On the exchange of momentum over the open ocean. *J. Phys. Oceanogr.*, **43**, 1589-1610, doi:10.1175/JPO-D-12-0173.1.

Emanuel, K., 2020: The relevance of theory for contemporary research in atmospheres, oceans, and climate. *AGU Adv*., **1**, doi:10.1029/2019AV000129.

Farrar, and Coauthors, 2020: S-MODE: The Sub-Mesoscale Ocean Dynamics Experiment. *IGARSS 2020-2020 IEEE International Geoscience and Remote Sensing Symposium*, Waikoloa, HI, IEEE, 3533-3536, doi:10.1109/IGARSS39084.2020.9323112.

Flexas, M. M., A. F. Thompson, H. S. Torres, P. Klein, J. T. Farrar, H. Zhang, and D. Menemenlis, 2019: Global estimates of the energy transfer from the wind to the ocean, with emphasis on near-inertial oscillations. *J. Geophys. Res.: Oceans*, **124**, 5723-5746, doi:10.1029/2018JC014453.

Fu, L. L., and R. Glazman, 1991: The effect of the degree of wave development on the sea state bias in radar altimetry measurement. *J. Geophys. Res.: Oceans*, **96**, 829-834, doi:10.1029/90JC02319.

Gentemann, C. L., and Coauthors, 2020: FluxSat: Measuring the ocean–atmosphere turbulent exchange of heat and moisture from space. *Remote Sens*., **12**, doi:10.3390/rs12111796.

Goldberg, E., 2019: Earth science has a whiteness problem. New York Times, https://www.nytimes.com/2019/12/23/science/earth-science-diversity-education.html.

Grare, L., W. L. Peirson, H. Branger, J. W. Walker, J. P. Giovanangeli, and V. Makin, 2013: Growth and dissipation of wind-forced, deep-water waves. *J. Fluid Mech.*, **722**, 5-50, doi:10.1017/jfm.2013.88.

Grare, L., N. M. Statom, N. Pizzo, and L. Lenain, 2021: Instrumented Wave Gliders for air-sea interaction and upper ocean research. *Front. Mar. Sci.*, **8**, doi:10.3389/fmars.2021.664728.

Janssen, P., 2004: *The interaction of ocean waves and wind*. Cambridge University Press, 300 pp.

Jullien, S., S. Masson, V. Oerder, G. Samson, F. Colas, and L. Renault, 2020: Impact of ocean–atmosphere current feedback on ocean mesoscale activity: Regional variations and sensitivity to model resolution. *J. Climate*, **33**, 2585-2602, doi:10.1175/JCLI-D-19-0484.1.

Kenyon, K. E., 1971: Wave refraction in ocean currents. *Deep Sea Res. Oceanogr. Abstr.*, **18**, 1023-1034, doi:10.1016/0011-7471(71)90006-4.

Kudryavtsev, V., M. Yurovskaya, B. Chapron, F. Collard, and C. Donlon, 2017: Sun glitter imagery of ocean surface waves. Part 1: Directional spectrum retrieval and validation. *J. Geophys. Res.: Oceans*, **122**, 1369-1383, doi:10.1002/2016JC012425.

Laughton, A. S., W. J. Gould, M. J. Tucker, and H. Roe 2010: *Of seas and ships and scientists: The remarkable history of the UK National Institute of Oceanography 1949-1973*. Lutterworth Press, 360 pp.

Lenain, L., and W. K. Melville, 2017: Measurements of the directional spectrum across the equilibrium saturation ranges of wind-generated surface waves. *J. Phys. Oceanogr.*, **47**, 2123-2138, doi:10.1175/JPO-D-17-0017.1.

Lenain, L., and N. Pizzo, 2021: Modulation of surface gravity waves by internal waves. *J. Phys. Oceanogr.,* **51**, 2735-2748, doi:10.1175/JPO-D-20-0302.1.

Lewis, D. M., S. E. Belcher, 2004: Time-dependent, coupled, Ekman boundary layer solutions incorporating Stokes drift. *Dyn. Atmos. Oceans*, **37**, 313-351, doi:10.1016/j.dynatmoce.2003.11.001.

Li, Q., A. Webb, B. Fox-Kemper, A. Craig, G. Danabasoglu, W. G. Large, and M. Vertenstein, 2016: Langmuir mixing effects on global climate: WAVEWATCH III in CESM. *Ocean Model*., **103**, 145-160, doi:10.1016/j.ocemod.2015.07.020.

Longuet-Higgins, M. S., 1962: The directional spectrum of ocean waves, and processes of wave generation. *Proc. Roy. Soc. London, Ser. A*, **265**, 286-315, doi:10.1098/rspa.1962.0010.

Marechal, G., and F. Ardhuin, 2021: Surface currents and significant wave height gradients: Matching numerical models and high-resolution altimeter wave heights in the Agulhas current region. *J. Geophys. Res.: Oceans*, **126**, doi:10.1029/2020JC016564.

McWilliams, J. C., and J. M. Restrepo, 1999: The wave-driven ocean circulation. *J. Phys. Oceanogr.*, **29**, 2523-2540, doi:10.1175/1520-0485(1999)029<2523:TWDOC>2.0.CO;2.

McWilliams, J. C., J. M. Restrepo, and E. M. Lane, 2004: An asymptotic theory for the interaction of waves and currents in coastal waters. *J. Fluid Mech.*, **511**, 135-178, doi:10.1017/S0022112004009358.

McWilliams, J. C., 2016: Submesoscale currents in the ocean. *Proc. Roy. Soc. London, Ser. A*, **472**, doi:10.1098/rspa.2016.0117.

Melville, W. K., 1996: The role of surface-wave breaking in air-sea interaction. *Annu. Rev. Fluid Mech.*, **28**, 279-321, doi:10.1146/annurev.fl.28.010196.001431.

Melville, W. K., F. C. Felizardo, and P. Matusov, 2004: Wave slope and wave age effects in measurements of electromagnetic bias. *J. Geophys. Res.: Oceans*, **109**, doi:10.1029/2002JC001708.

Melville, W. K., R. H. Stewart, W. C. Keller, J. A. Kong, D. V. Arnold, A. T. Jessup, M. R. Loewen, and A. M. Slinn, 1991. Measurements of electromagnetic bias in radar altimetry. *J. Geophys. Res.: Oceans*, **96**, 4915-4924, doi:10.1029/90JC02114.

Peral, E., S. Tanelli, Z. Haddad, O. Sy, G. Stephens, and E. Im, 2015: Raincube: A proposed constellation of precipitation profiling radars in CubeSat. *2015 IEEE International Geoscience and Remote Sensing Symposium (IGARSS)*, Milan, Italy, IEEE, 1261-1264, doi:10.1109/IGARSS.2015.7326003.

Phillips, O. M., 1977: *The dynamics of the upper ocean*. Cambridge University Press, 344 pp.

Phillips, O. M., 1984: On the response of short ocean wave components at a fixed wavenumber to ocean current variations. *J. Phys, Oceanogr.*, **14**, 1425-1433, doi:10.1175/1520-0485(1984)014<1425:OTROSO>2.0.CO;2.

Phillips, W. R. C., 2002: Langmuir circulations beneath growing or decaying surface waves. *J. Fluid Mech.*, **469**, 317-342, doi:10.1017/S0022112002001908.

Pizzo, N., W. K. Melville, and L. Deike, 2019: Lagrangian transport by nonbreaking and breaking deep-water waves at the ocean surface. *J. Phys. Oceanogr.*, **49**, 983-992, doi:10.1175/JPO-D-18-0227.1.

Pizzo, N., and R. Salmon, 2021: Particle description of the interaction between wave packets and point vortices. *J. Fluid Mech.*, **925**, doi:10.1017/jfm.2021.661.

Quilfen, Y., M. Yurovskaya, B. Chapron, and F. Ardhuin, 2018: Storm waves focusing and steepening in the Agulhas current: Satellite observations and modeling. *Remote Sens. Environ.*, **216**, 561-571, doi:10.1016/j.rse.2018.07.020.

Quilfen, Y., and B. Chapron, 2019: Ocean surface wave-current signatures from satellite altimeter measurements. *Geophys. Res. Lett.*, **46**, 253-261, doi:10.1029/2018GL081029.

Rapizo, H., T. H. Durrant, and A. V. Babanin, 2018: An assessment of the impact of surface currents on wave modeling in the Southern Ocean. *Ocean Dyn.*, **68**, 939-955, doi:10.1007/s10236-018-1171-7.

Rascle, N., B. Chapron, A. Ponte, F. Ardhuin, and P. Klein, 2014: Surface roughness imaging of currents shows divergence and strain in the wind direction. *J. Phys. Oceanogr.*, **44**, 2153-2163, doi:10.1175/JPO-D-13-0278.1.

Rascle, N., F. Nouguier, B. Chapron, A. Mouche, and A. Ponte, 2016: Surface roughness changes by finescale current gradients: Properties at multiple azimuth view angles. *J. Phys. Oceanogr.*, **46**, 3681-3694, doi:10.1175/JPO-D-15-0141.1.

Renault, L., M. J. Molemaker, J. C. McWilliams, A. F. Shchepetkin, F. Lemarié, D. Chelton, S. Illig, and A. Hall, 2016: Modulation of wind work by oceanic current interaction with the atmosphere. *J. Phys. Oceanogr.*, **46**, 1685-1704, doi:10.1175/JPO-D-15-0232.1.

Renault, L., J. C. McWilliams, and S. Masson, 2017: Satellite observations of imprint of oceanic current on wind stress by air-sea coupling. *Sci. Rep.*, **7**, doi:10.1038/s41598-017-17939-1.

Rodríguez, E., M. Bourassa, D. Chelton, J. T. Farrar, D. Long, D. Perkovic-Martin, and R. Samelson, 2019: The Winds and Currents Mission concept. *Front. Mar. Sci.*, **6**, doi:10.3389/fmars.2019.00438.

Romero, L., 2019: Distribution of surface wave breaking fronts. *Geophys. Res. Lett.*, **46**, 10463-10474, doi:10.1029/2019GL083408.

Romero, L., D. Hypolite, and J. C. McWilliams, 2020: Submesoscale current effects on surface waves. *Ocean Model*., **153**, doi:10.1016/j.ocemod.2020.101662.

Sarmiento, J. L., and N. Gruber, 2006: *Ocean biogeochemical dynamics*. Princeton University Press, 504 pp.

Shrira, V. I., and R. B. Almelah, 2020: Upper-ocean Ekman current dynamics: A new perspective. *J. Fluid Mech.*, **887**, doi:10.1017/jfm.2019.1059.

Smith, J. A., 1992: Observed growth of Langmuir circulation. *J. Geophys. Res.: Oceans*, **97**, 5651-5664, doi:10.1029/91JC03118.

Stewart, R. H., and J. W. Joy, 1974: HF radio measurements of surface currents. *Deep Sea Res. Oceanogr. Abstr.*, **21**, 1039-1049, doi:10.1016/0011-7471(74)90066-7.

Sullivan, P. P., J. C. McWilliams, and W. K. Melville, 2007: Surface gravity wave effects in the oceanic boundary layer: Large-eddy simulation with vortex force and stochastic breakers. *J. Fluid Mech.*, **593**, 405-452, doi:10.1017/S002211200700897X.

Sullivan, P. P., and J. C. McWilliams, 2010: Dynamics of winds and currents coupled to surface waves. *Annu. Rev. Fluid Mech.*, **42**, 19-42, doi:10.1146/annurev-fluid-121108-145541.

Suzuki, N., 2019: On the physical mechanisms of the two-way coupling between a surface wave field and a circulation consisting of a roll and streak. *J. Fluid. Mech.*, **881**, 906-950, doi:10.1017/jfm.2019.752.

van Sebille, E., and Coauthors, 2020: The physical oceanography of the transport of floating marine debris. *Environ. Res. Lett.*, **15**, doi:10.1088/1748-9326/ab6d7d.

Verdy, A., M. R. Mazloff, B. D. Cornuelle, and S. Y. Kim, 2014: Wind-driven sea level variability on the California coast: An adjoint sensitivity analysis. *J. Phys. Oceanogr.*, **44**, 297-318, doi:10.1175/JPO-D-13-018.1.

Veron, F., 2015: Ocean spray. *Annu. Rev. Fluid Mech.*, **47**, 507-538, doi:10.1146/annurev-fluid-010814-014651.

Villas Bôas, A. B., and Coauthors, 2019: Integrated observations of global surface winds, currents, and waves: Requirements and challenges for the next decade. *Front. Mar. Sci.*, **6**, doi:10.3389/fmars.2019.00425.

Villas Bôas, A. B., and W. R. Young, 2020: Directional diffusion of surface gravity wave action by ocean macroturbulence. *J. Fluid Mech.*, **890**, doi:10.1017/jfm.2020.116.

Villas Bôas, A. B., B. D. Cornuelle, M. R. Mazloff, S. T. Gille, and F. Ardhuin, 2020: Wave–current interactions at meso-and submesoscales: Insights from idealized numerical simulations. *J. Phys. Oceanogr.*, **50**, 3483-3500, doi:10.1175/JPO-D-20-0151.1.

Wang, D., T. Kukulka, B. G. Reichl, T. Hara, and I. Ginis, 2019: Wind–wave misalignment effects on Langmuir turbulence in tropical cyclone conditions. *J. Phys. Oceanogr.*, **49**, 3109-3126, doi:10.1175/JPO-D-19-0093.1.

Wilkinson, M. D., and Coauthors, 2016: The FAIR Guiding Principles for scientific data management and stewardship. *Sci. Data*, **3**, doi:10.1038/sdata.2016.18.

Yu, Y., D. T. Sandwell, S. T. Gille, and A. B. Villas Bôas, 2021: Assessment of ICESat-2 for the recovery of ocean topography. *Geophys. J. Int.*, **226,** 456-467, doi:10.1093/gji/ggab084.

Yurovskaya, M., V. Kudryavtsev, B. Chapron, and F. Collard, 2019: Ocean surface current retrieval from space: The Sentinel-2 multispectral capabilities. *Remote Sens. Environ*., **234**, doi:10.1016/j.rse.2019.111468.

Current feedback to the atmosphere: Implications for ocean dynamics, air-sea interactions, and modeling

Qi Shi

I. M. Systems Group, Inc.

The western boundary current (WBC) systems are featured with strong ocean current, prominent mesoscale eddies, and large sea surface temperature (SST) gradient. Over the WBC region, the ocean drives the atmosphere motions on the mesoscale, which have a significant impact on local atmospheric conditions, regional to basin-scale climate, and biogeochemical dynamics (Kelly et al. 2001; Chelton et al. 2004; Minobe et al. 2008; Chelton and Xie 2010; O'Neil et al. 2010). Ocean currents modify wind stress by changing the wind shear between the ocean and atmosphere. In a fully coupled ocean-atmospheric system, the change of wind stress and its curl feeds back to the ocean by modifying the horizontal advection and vertical motion in the upper ocean. The impact of current-stress coupling on the dynamics and thermodynamics of the marine atmospheric boundary layer (MABL) can be amplified in ocean frontal areas (Shi and Bourassa 2019), where SST and its gradient are also highly coupled with wind stress locally (Xie 2004; Small et al. 2008). The presence of waves adds to the complexity of the current feedback to the atmosphere by wave-current interaction and wave-induced vertical mixing. Using surface winds observed by scatterometers and sea surface heights observed by altimeters, Gaube et al. (2015) found that current-induced Ekman pumping velocities in the interior of mesoscale ocean eddies approach O(10) cm day^{-1}. Due to the long time scale of current variation, missing current-wind interactions in numerical models leads to substantial biases in air-sea fluxes (Edson et al. 2013) and SST (Wang et al. 2014; Zuidema et al. 2016) near the WBC region.

Current-stress coupling

On large scale (~100 km), ocean currents are driven by wind stress resulting in an approximate balance between the pressure gradient force and the Coriolis force. Currents modify the wind stress by changing the wind shear between ocean surface and atmosphere:

$$\tau = \rho_a C_D \left| \vec{U}_{wind} - \vec{U}_{current} \right| (\vec{U}_{wind} - \vec{U}_{current})$$

where τ is wind stress, ρ_a is air density, C_D is drag coefficient, $\vec{U}_{wind}$ is 10-m wind, $\vec{U}_{current}$ is the surface current.

Traditionally, ocean currents are neglected in wind stress calculations because they are usually one-order magnitude smaller than the surface wind (Wu 1975). However, recent studies using high-resolution models report that ocean current can substantially reduce wind stress (up to 30%) and eddy kinetic energy (EKE, up to 42%) near strong currents and mesoscale eddies (Dawe and Tompson 2006; Hutchinson et al. 2010; Munday and Zhai 2015; Seo et al. 2016; Song et al. 2020). The EKE reduction is not limited to the surface layer—it can penetrate up to 1000 m depth under water (Song et al. 2020). The currents-stress coupling also modifies the curl of the wind stress and creates current-inducted vertical velocity, which may impact the biogeochemical processes in the upper ocean.

Current-wave-stress coupling

Waves change surface roughness and have a substantial impact on air-sea momentum exchange (Taylor and Yelland 2001; Drennan et al. 2005; Moon et al. 2004 a,b). Waves can also pass the momentum to currents through wave breaking, wave-wave, and wave-current interaction. Shi and Bourassa (2019) provides a detailed analysis of oceanic and atmospheric response to the current-wave-stress interaction around the Gulf Stream using a high-resolution ocean-wave-atmosphere full coupled modeling system. In this three-way coupled modeling system, ocean currents and wave characteristics are directly obtained from the ocean/wave model and explicitly used in the surface momentum calculation. Moreover, air-sea heat fluxes cannot only be directly influenced by surface currents and waves through changing the surface roughness length but also indirectly influenced by surface currents and waves through changes in SST and related changes induced in the atmospheric boundary layer. In which case, the model represents the air-sea interaction in a more realistic fashion. Coupling current, wave, and stress simultaneously leads to a 15% increase in the monthly-mean wind stress near the Cape Hatteras (Shi and Bourassa 2019). Ekman pumping velocity changes in response to wind stress changes are found along the Gulf Stream with magnitudes exceeding 0.4 m/day. Inside the Gulf Stream, wave-current interaction increases significant wave height. Outside the Gulf Stream, the current effect offsets the wave effect on wind stress. Adding wave effect increases the coupling coefficient between surface wind and SST by 17% and results in a more realistic stress pattern compared to the satellite observation. The considerable change in the wind stress and its curl due to current-wave-stress coupling leads to substantial changes in SST (~ 1°C) and ocean current (~0.2 m/s) response patterns at the Gulf Stream, which are collocated near the SST frontal regional in the shape of warm/cold-core eddies. These changes in wind and SST have impacts on air-sea heat fluxes. Considerable changes of latent heat flux over 20 W/m^2 and sensible heat flux over 5 W/m^2 are found over the Gulf Stream. Shi and Bourassa (2019) found the sensitivity of the curl of wind stress on the current decreases with increasing grid spacing. High-resolution observations (~5 km) of wind and currents are needed to observe this kind of coupling (Bourassa et al. 2019).

Feedback mechanism

Figure 1 summarizes the current-wave-stress feedback mechanism in MABL. Wind stress drives waves and currents. Currents feed back to wind stress by modifying wind shear between the ocean and the atmosphere. Wave-current interaction increases significant wave height inside the Gulf Stream (Ponce de León and Guedes Soares 2021). Growing/decaying waves change surface roughness and impact the momentum exchange between the ocean and the atmosphere. Changes in wind stress and its curl have a substantial impact on the horizontal current-advection and vertical velocity in the upper ocean. Differential horizontal advection and vertical entrainment are two dominant processes that lead to considerable SST change in the Gulf Stream (Shi and Bourassa 2019). Waves also impact SST by increasing vertical mixing and mixed layer depth (Bruneau et al. 2018). On larger spatial scales (>25 km), both observational and modeling studies (Chelton et al. 2004; Small et al. 2008; O'Neill et al. 2010; Schneider and Qiu 2015) have found that SST modifies surface wind in persistent SST frontal regions. Over the warmer side of an SST front, surface wind speed increases with the unstable atmospheric boundary layer. High wind momentum from above descends to the surface by

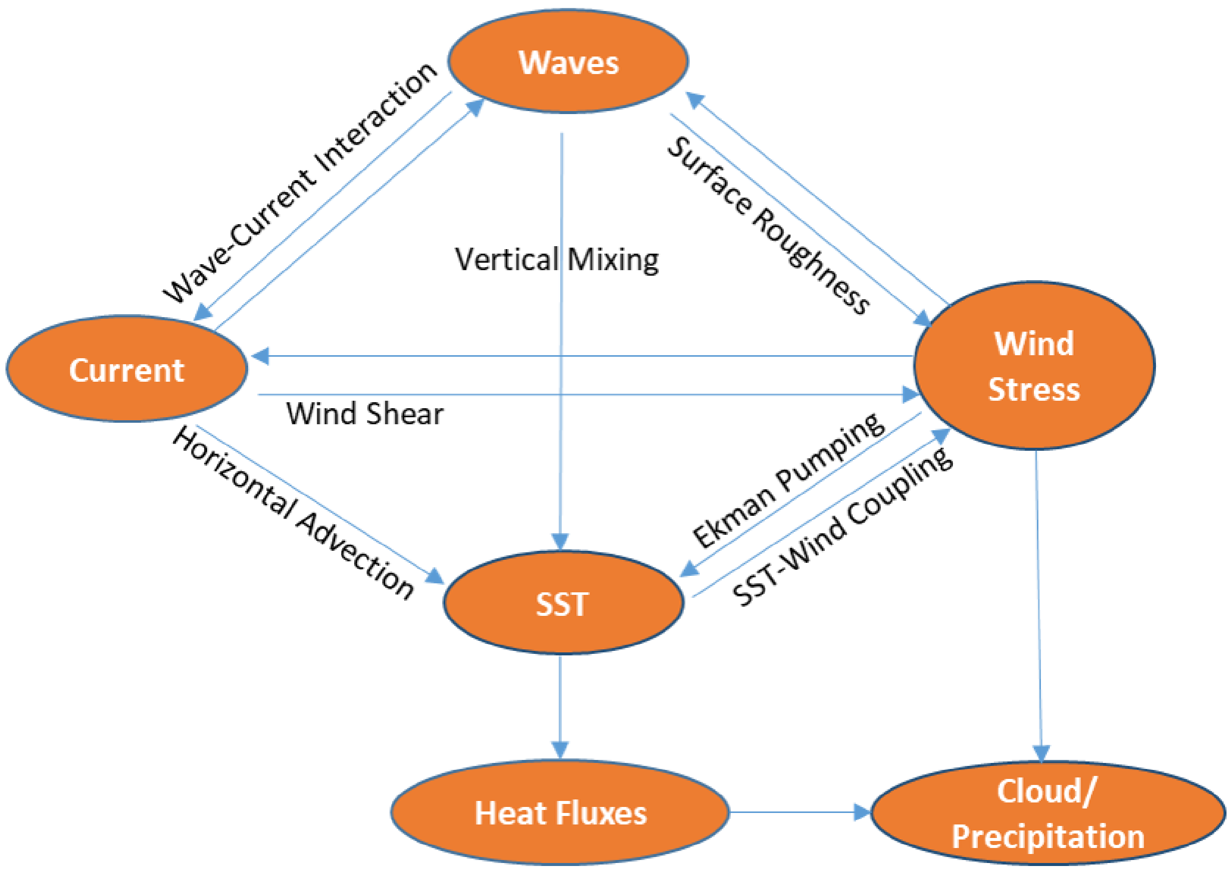

Figure 1. Schematic diagram of the feedback mechanism in coupling ocean currents, waves, and wind stress simultaneously.

vertical mixing and increases the surface wind speed. On the colder side of an SST front, surface wind speed decreases with increased boundary layer stability. The secondary circulation induced by the local pressure gradient crossing an SST front also contributes to surface wind changes. Since SST is coupled to the MABL, the warming/cooling of SST changes the air temperature and, therefore, changes the pressure gradient near the surface as well as the turbulent vertical mixing, which feed back to the surface wind. SST also influences saturation vapor pressure and boundary-layer stability over the ocean surface, which changes the evaporation over the ocean surface. This evaporation change can further impact precipitation and cloud formation/ radiation in the atmosphere.

Although the results discussed in this article focus on the Gulf Stream region, similar impact of current-wind interaction on the MABL is found over Kuroshio (Takatama and Schneider 2016), California Current System (Seo et al. 2016), and Southern Ocean (Song et al. 2020). These high-resolution model studies have improved our understanding of current-stress coupling on the dynamics and thermodynamics of the MABL. They also point out new questions and challenges. For example, temporal- and spatial-resolution of observation need to be improved to validate the mesoscale coupling from numerical model. The impact of current-wave-stress coupling on precipitation and biogeochemical processes need to be quantified.

References

Bourassa, M. A., and Coauthors, 2019: Remotely sensed winds and wind stresses for marine forecasting and ocean modeling. *Front. Mar. Sci.,* **6**, doi:10.3389/fmars.2019.00443.

Bruneau, N., R. Toumi, and S. Wang, 2018: Impact of wave whitecapping on land falling tropical cyclones. *Sci. Rep.*, **8**, doi:10.1038/s41598-017-19012-3.

Chelton, D. B., M. G. Schlax, M. H. Freilich, and R. F. Milliff, 2004: Satellite measurements reveal persistent small-scale features in ocean winds. *Science*, **303**, 978-983, doi:10.1126/science.1091901.

Chelton, D. B., and S.-P. Xie, 2010: Coupled ocean-atmosphere interaction at oceanic mesoscales. *Oceanography*, **23**, 52–69, doi:10.5670/oceanog.2010.05.

Dawe, J. T., and L. A. Thompson, 2006: Effect of ocean surface currents on wind stress, heat flux, and wind power input to the ocean. *Geophys. Res. Lett.*, **33**, doi:10.1029/2006GL025784.

Drennan, W. M., P. K. Taylor, and M. J., 2005: Parameterizing the sea surface roughness. *J. Phys. Oceanogr.*, 35, 835–848, doi:10.1175/JPO2704.1.

Edson, J. B., and Coauthors, 2013: On the exchange of momentum over the open ocean. *J. Phys. Oceanogr.*, **43**, 1589–1610, doi:10.1175/JPO-D-12-0173.1.

Gaube, P., D. B. Chelton, R. M. Samelson, M. G. Schlax, and L. W. O'Neill, 2015: Satellite observations of mesoscale eddy-induced Ekman pumping. *J. Phys. Oceanogr.*, **45**, 104–132, doi:10.1175/JPO-D-14-0032.1.

Hutchinson, D. K., A. M. C. Hogg, and J. R. Blundell, 2010: Southern Ocean response to relative velocity wind stress forcing. *J. Phys. Oceanogr.*, **40**, 326–339, doi:10.1175/2009JPO4240.1.

Kelly, K. A., S. Dickinson, M. J. McPhaden, and G. C. Johnson, 2001: Ocean currents evident in satellite wind data. *Geophys. Res. Lett.*, **28**, 2469–2472, doi:10.1029/2000GL012610.

Minobe, S., A. Kuwano-Yoshida, N. Komori, S.-P. Xie, and R. J. Small, 2008: Influence of the Gulf Stream on the troposphere. *Nature*, **452**, 206-209, doi:10.1038/nature06690.

Moon, I.-J., T. Hara, I. Ginis, S. E. Belcher, and H. L. Tolman, 2004: Effect of surface waves on air–sea momentum exchange. Part I: Effect of mature and growing seas. *J. Atmos. Sci.*, **69**, 2321–2333, doi:10.1175/1520-0469(2004)061<2321:EOSWOA>2.0.CO;2.

Moon, I-J., I. Ginis, and T. Hara, 2004: Effect of surface waves on air–sea momentum exchange. Part II: Behavior of drag coefficient under tropical cyclones. *J. Atmos. Sci*, **61**, 2334–2348, doi:10.1175/1520-0469(2004)061<2334:EOSWOA>2.0.CO;2.

Munday, D. R., and X. Zhai, 2015: Sensitivity of Southern Ocean circulation to wind stress changes: Role of relative wind stress. *Ocean Model.,* **95**, 15–24, doi:10.1016/j.ocemod.2015.08.004.

O'Neill, L. W., S. K. Esbensen, N. Thum, R. M. Samelson, and D. B. Chelton, 2010: Dynamical analysis of the boundary layer and surface wind responses to mesoscale SST perturbations. *J. Climate*, 23, 559–581, doi:10.1175/2009JCLI2662.1.

Ponce de León, S. and C. Guedes Soares, 2021: Numerical modelling of the effects of the Gulf Stream on the wave characteristics. *J. Mar. Sci. Eng.*, **9**, 1–15, doi:10.3390/jmse9010042.

Schneider, N., and B. Qiu, 2015: The atmospheric response to weak sea surface temperature fronts. *J. Atmos. Sci.*, **72**, 3356–3377, doi:10.1175/JAS-D-14-0212.1.

Seo, H., A. J. Miller, and J. Norris, 2016: Eddy–wind interaction in the California Current System: Dynamics and impacts. *J. Phys. Oceanogr.*, **46**, 439–459, doi:10.1175/JPO-D-15-0086.1.

Shi, Q., and M. A. Bourassa, 2019: Coupling ocean currents and waves with wind stress over the Gulf Stream. *Remote Sens.*, **11**, 1476, doi:10.3390/rs11121476.

Small, R. J., and Coauthors, 2008: Air-sea interaction over ocean fronts and eddies. *Dyn. Atmos. Oceans*, **45**, 274–319, doi:10.1016/j.dynatmoce.2008.01.001.

Song, H., J. Marshall, D. J. McGillicuddy, and H. Seo, 2020: Impact of current-wind interaction on vertical processes in the Southern Ocean. *J. Geophys. Res.: Oceans*, **125**, doi:10.1029/2020JC016046.

Taylor, P. K., and M. J. Yelland, 2001: The dependence of sea surface roughness on the height and steepness of the waves. *J. Phys. Oceanogr.*, **31**, 572–590, doi:10.1175/1520-0485(2001)031<0572:TDOSSR>2.0.CO;2.

Takatama, K., and Schneider, N., 2017: The role of back pressure in the atmospheric response to surface stress induced by the Kuroshio. *J. Atmos. Sci*, **74**, 597–615, doi:10.1175/JAS-D-16-0149.1

Wang, C., L. Zhang, S.-K. Lee, L. Wu, and C. R. Mechoso, 2014: A global perspective on CMIP5 climate model biases. *Nat. Climate Chang.*, **4**, 201–205, doi:10.1038/nclimate2118.

Wu, J., 1975: Wind-induced drift currents. *J. Fluid Mech.*, **68**, 49-70, doi:10.1017/S0022112075000687.

Xie, S.-P., 2004: Satellite observations of cool ocean-atmosphere interaction. *Bull. Amer. Meteor. Soc.*, **85**, 195-208 doi:10.1175/BAMS-85-2-195.

Zuidema, P., and Coauthors, 2016: Challenges and prospects for reducing coupled climate model SST biases in the eastern tropical Atlantic and Pacific Oceans: The U.S. CLIVAR Eastern Tropical Oceans Synthesis Working Group, *Bull. Amer. Meteor. Soc.*, **97**, 2305–2328, doi:10.1175/BAMS-D-15-00274.1.

Forecasting currents: Approaches and challenges for data assimilation and modeling

Matthew J. Carrier, Scott R. Smith, Robert E. Helber, Gregg A. Jacobs, and Hans Ngodock

US Naval Research Laboratory, Stennis Space Center

Ocean currents are responsible for the transport of heat from equatorial regions to the polar regions, transport of fresh water runoff from rivers and ice melt, and transport of pollutants in the ocean, such as hydrocarbons. Accurate prediction of ocean currents is vital for predicting these phenomena, as well as at-sea search and rescue operations and other drift prediction applications.

As operational ocean modeling has advanced in capability, researchers have sought to improve ocean current prediction through higher-resolution modeling and data assimilation. Data assimilation is vital to constraining the ocean model circulation and has been an area of active research for more than twenty years. Currently, operational ocean modeling relies heavily upon satellite sea surface height (SSH) observations. These observations provide models with information regarding the dynamic topography of the ocean, which helps models constrain large-scale ocean currents through the geostrophic relationship. There are limitations with this approach, however, as satellite altimeters provide observations in a narrow path along the satellite ground track. This produces large gaps in SSH observation coverage during any analysis cycle, which strongly inhibit the spatial scales that can be constrained by models (Souopgui et al. 2020). This leads to misplaced and misshapen ocean fronts and eddies, which lead to error in ocean current prediction. Much research has been done in assimilating ocean current observations into ocean models to improve ocean current prediction.

Previous work on ocean current observation assimilation

Early work in ocean current assimilation focused on simpler techniques, such as nudging (Fan et al. 2004), to more complex methods, such as variational data assimilation (Taillandier et al. 2006). More recent studies have continued to use variational data assimilation techniques, such as the four-dimensional variational (4DVAR) method (Powell et al. 2008; Carrier et al. 2014; Muscarella et al. 2015; Phillipson and Toumi 2017; Phillipson et al. 2021), or ensemble methods, such as the Ensemble Kalman Filter (ENKF, Coelho et al. 2015) or the Local Ensemble Transform Kalman Filter (LETKF) using an augmented state approach (Sun and Penny 2019). Just as there are many methods of data assimilation used in ocean current assimilation, the form of the ocean current observations are equally as varied. These include (but are not limited to) Acoustic Doppler Current Profilers (ADCP), which provide point-wise profiles of ocean currents; High-Frequency (HF) radars, which provide estimates of surface ocean currents; derived currents from satellite altimetry (Le Traon et al. 2015); and surface drifters. Surface drifters are normally treated in two ways for purposes of data assimilation: either as position observations (the "Lagrangian" approach) or to derive ocean velocity estimates via the position change over time of the drifter (the "Eulerian" approach). The Eulerian approach has been utilized in many studies (Hernandez et al. 1995; Ishikawa et al. 1996; Toner et al. 2001; Carrier et al. 2014; Coelho et al. 2015; Muscarella et al. 2015; Phillipson and Toumi 2017; Santoki et al. 2012), while the Lagrangian approach has been applied in other studies as well (Ide et al. 2002; Kuznetsov et al. 2003; Molcard et al. 2003; Ozgokmen et al. 2003; Taillandier et al. 2006; Nilsson et al. 2012; Sun and Penny 2019).

Ocean current observations: Types and challenges

Each type of ocean current observation has its own challenges in regards to data assimilation. Examined here are two of the observation types: HF radar data and surface drifters. HF radars provide "maps" of ocean current measurements rather than a point-wise measurement, such as ADCPs or surface drifters. They do this by analyzing a backscattering radio wave emitted from a radar, where the radio waves are reflected back to the radar by surface ocean waves. The movement of the surface ocean waves (via the surface current) will produce a Doppler shift of the returning energy; it is this Doppler shift that is exploited to derive estimates of the surface ocean current velocity. A single HF radar station is only capable of measuring the velocity that is directly in-line with the radar antenna. Therefore, it is common that many HF radar stations (at least two) will be used in order to derive suitable observations of the surface currents. Combining the observations of two or more stations can be done in a number of ways, such as through optimal interpolation techniques or two-dimensional variational (2DVAR) methods (Yaremchuk and Sentchev 2011).

Surface drifters are another data source that is growing in usage for collecting near-surface ocean current observations. There are many drifter designs, but they commonly possess a surface platform that houses various instruments, a battery pack, a Global Positioning System (GPS) device, and a transmitter. Drifters often use an underwater sail called a "drogue". Drogues are used with drifters in order to limit the effects of surface wind and wave action on the drifter's movement and help the drifter move mainly with the upper-ocean current. Drogues can be as deep as 15 m, such as those used in the Surface Velocity Program (SVP), or as shallow as CODE-type drifters (Davis 1985), with drogues as short as 1 m (Poje et al. 2014; Carrier et al. 2014).

There are many challenges in processing and assimilating drifter observations for ocean current prediction, some of which are tied to the way the observation is assimilated (i.e., as a Lagrangian or Eulerian observation). Regardless of the form, some processing is needed to ensure the drifter position and velocity present an accurate representation of the near-surface ocean current. The drogue that is attached to the drifter can detach, leading to a drifter that is forced mainly by the wind and wave action at the ocean's surface. Also, individuals on fishing boats will often retrieve drifters from the ocean and return them to shore. These types of behaviors can be determined by examining the drifter trajectories, their behavior relative to nearby drifters, and any acceleration the drifter may exhibit. When drifters are used to estimate Eulerian velocity, some considerations must be made to whether the drifter data set is appropriate for such a calculation. Molcard et al. (2005) suggest that derivation of Eulerian velocity from drifters can become problematic if the sampling period exceeds the Lagrangian time scale, which is typically 1-3 days for ocean surface velocity and 7-15 days for the deep interior. In addition, drifters are subject to accelerations due to tides and inertial oscillations. The latter signal can be removed by computing velocities from drifters that are separated on the same time scale as the inertial period. When this is done, it is important to compute the average model background velocity over the same time scale when computing the model-observation innovation. This ensures that the low-frequency motion (geostrophic velocity), and not the high-frequency motion, is corrected.

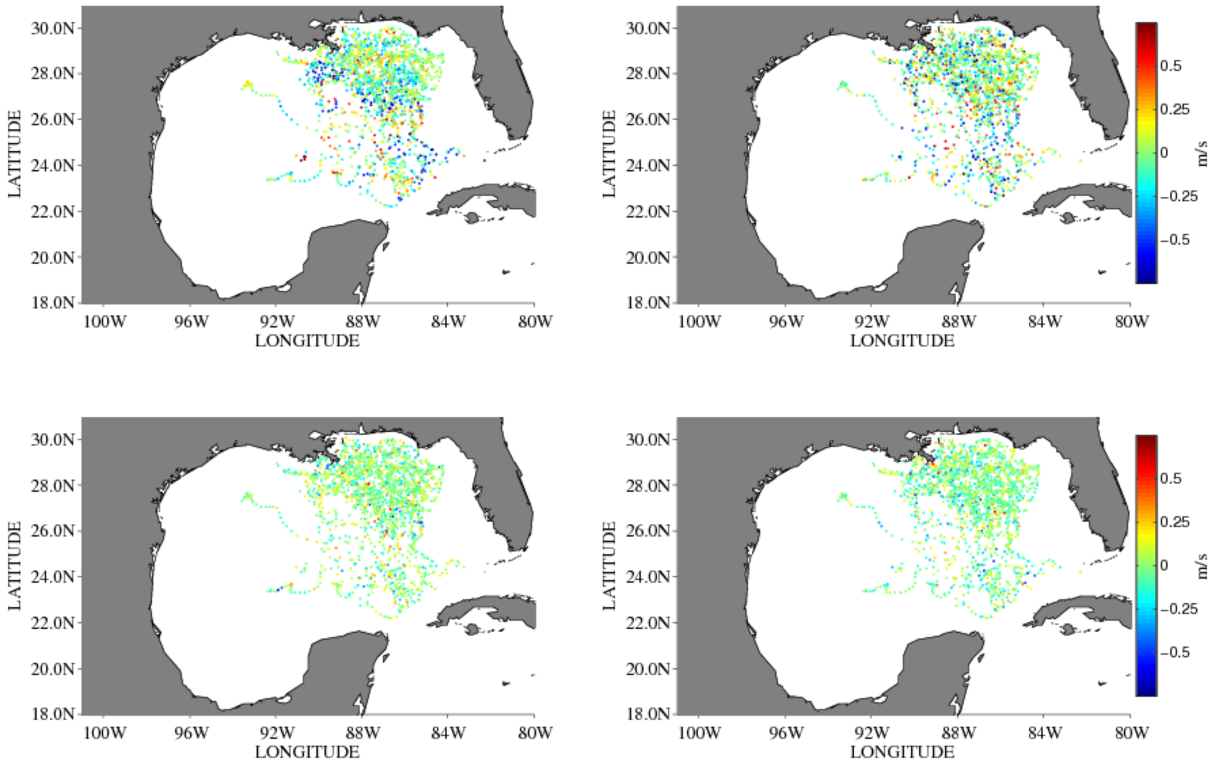

Figure 1. All assimilated drifter-derived velocities from 1 August 2012 through 30 September 2012 for the u-component (left panels) and v-component (right panels) from the model "first guess" fields (top panels) and the model analysis fields (bottom panels). Figure from Carrier et al. (2014).

Data assimilation methods used for ocean current observation assimilation

Methods for assimilating ocean current observations vary widely. However, they all attempt to include a multivariate adjustment of the entire ocean field due to the assimilation of ocean current observations. Large-scale ocean currents are the dynamical response of the ocean to the pressure gradient and Coriolis forces. As such, when correcting the ocean model velocity field, it is vital to simultaneously update the thermodynamic structure of the underlying ocean. To do this, the background error covariance used in the assimilation process must contain appropriate dynamical balance constraints. With three-dimensional variational (3DVAR) techniques, this can be achieved by building a dynamical balance operator into the background error covariance. This can take the form of a balance operator based on linearized dynamics (Weaver et al. 2005) or through the use of empirically-derived vertical error covariances (based on observations) that relate temperature and salinity to velocity through geopotential height (Helber et al. 2013). The 4DVAR technique is able to directly assimilate ocean current observations due to its reliance on the tangent linear and adjoint models to form its four-dimensional background error covariance (Ngodock and Carrier 2014; Carrier et al. 2016). The tangent linear and adjoint models provide a multivariate background error covariance through the linearized dynamical balance relationships inherent in their design. Ensemble methods, such as the EnKF and LETKF (Coelho et al. 2015; Sun and Penny 2019), rely on the ensemble of forecast states to build the dynamically-balanced background error covariance.

Selected applications: US Navy assimilation and modeling using 3DVAR and 4DVAR

Carrier et al. (2014) sought to assimilate drifter-derived

Eulerian ocean current observations from a drifter deployment in the Gulf of Mexico in 2012 known as the Grand LAgrangian Deployment (GLAD; Poje et al. 2014; Carrier et al. 2014). In this work, Carrier et al. (2014) employed the Navy Coastal Ocean Model (NCOM) 4DVAR to assimilate the drifter-derived velocities from 1 August 2012 through 30 September 2012. The drifter trajectories were filtered using the methods described in Carrier et al. (2014) and Coelho et al. (2015) for unrealistic accelerations and inertial oscillations. Results of this work showed great promise in not only correcting the ocean velocity field at the analysis time (Figure 1), but also in projecting this correction forward into the forecast period. During one particular 96-hr forecast (Figure 2), the assimilation of velocity measurements constrains the model forecast to such a degree that the model drifter trajectories match very closely with the observed drifters. In addition to this, the underlying SSH structure has also been appropriately adjusted to support the new velocity field.

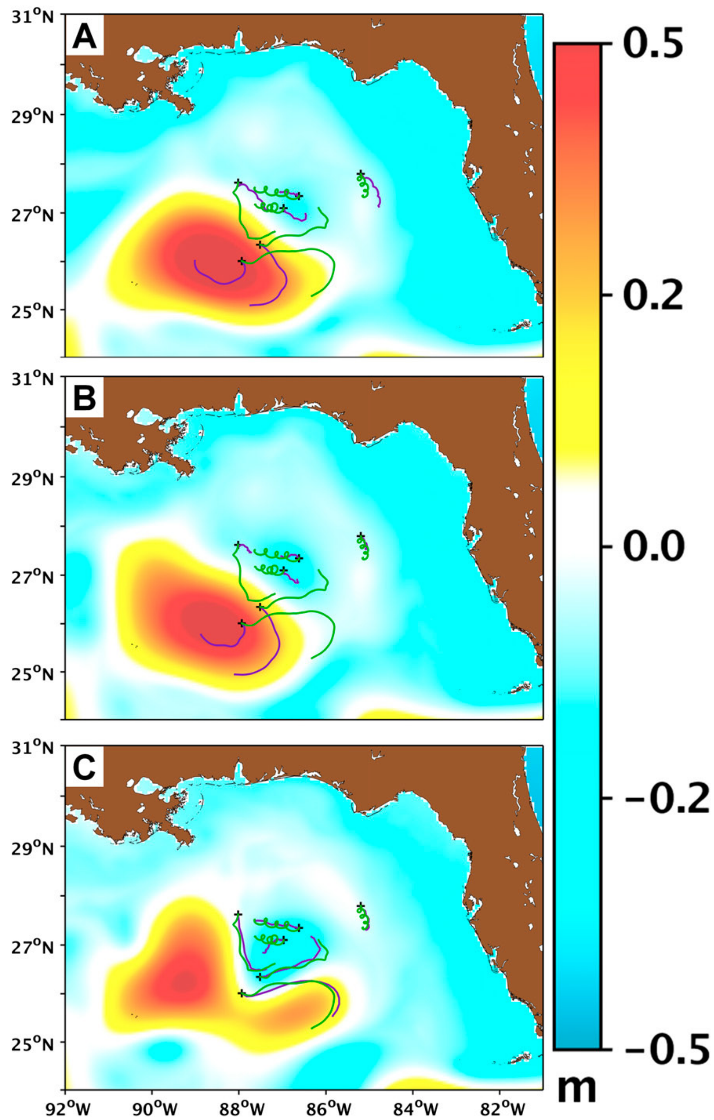

Figure 2. NCOM 96-hr forecast of SSH (color contours) and model velocity-advected drifters (purple lines) in the Northeast Gulf of Mexico for 21 August 2012. Model drifter trajectories are compared to observed drifter trajectories (green lines). Comparisons shown for NCOM model with (a) no assimilation, (b) temperature and salinity assimilation only, and (c) assimilation of temperature, salinity, and drifter-derived ocean current observations. Figure from Muscarella et al. (2015).

Another US Navy application of ocean current assimilation was conducted in the Gulf of Mexico, this time in support of a Defense Advanced Research Projects Agency (DARPA) project known as the "Ocean of Things". This effort uses the Navy Coupled Ocean Data Assimilation (NCODA) system with 3DVAR (Smith et al. 2021). Here, velocity observations are assimilated using a multivariate background error covariance embedded within the NCODA-3DVAR. This allows for cross-correlations between temperature and salinity to ocean current velocity through geopotential height using the Improved Synthetic Ocean Profile system vertical covariance structure. In this experiment, a series of drifters were released in the Gulf of Mexico in August, 2020. NCODA computes the Eulerian velocity from these drifter positions and those observations are assimilated into the 3DVAR, with subsequent 72-hr forecasts performed by NCOM. The experiment started on 15 August, with drifter-derived velocities available for assimilation starting on 29 August. Examining the results on 10 September shows that NCOM, through the 3DVAR assimilation of ocean current observations, is positioning the ocean currents and a mesoscale eddy in the correct locations in the vicinity of the velocity measurements (Figure 3). The result here are very similar to the previous 4DVAR work in that an eddy in the

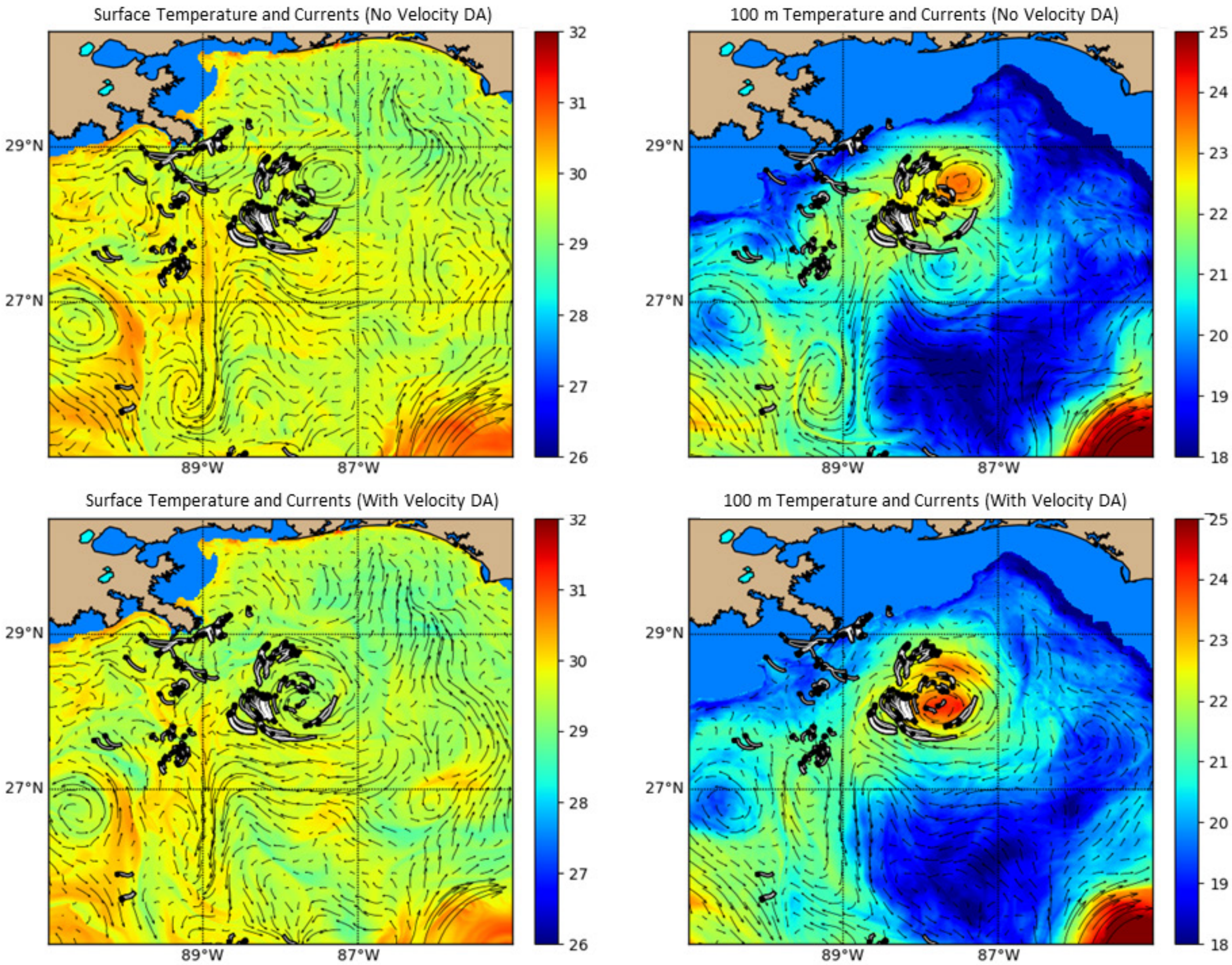

Figure 3. Results from NCOM model run with no assimilation (upper plots) and with ocean velocity assimilation using NCODA-3DVAR (bottom plots). Results shown for surface currents and temperatures (left plots) and for currents and temperatures at 100 m depth (right plots). Ocean drifter trajectories are indicated by curved white lines in each plot. The eddy in the vicinity of the drifters has been repositioned to the southwest by the 3DVAR assimilation of velocity observations (lower right panel near 28° N and 88° W). Figure in submission to *Ocean Modelling* as part of Smith et al. (2021).

vicinity of the drifter observations is repositioned by the assimilation of velocity measurements in NCODA-3DVAR. This, again, shows the utility of velocity observations to not only correct the ocean currents in the model, but the underlying thermodynamic structure as well.

Future directions

It has become apparent that ocean current observations provide a useful data set from which corrections can be made to the ocean model for large-scale motions as well as submesoscale phenomenon. Available ocean current observations, however, remain sparse in both space and time, thus making their impact in current operational modeling limited. Research is on-going to utilize profiling float trajectories from the ARGO program, and other sources, in order to expand the number of available ocean current observations. Efforts to collect surface ocean current observations from space are also a possibility. NASA's Surface Water and Ocean Topography (SWOT) mission, launching in 2022, will provide wide-swath altimeter observations. Deriving geostrophic surface currents from this data may be possible and is being investigated. Also, the European Space Agency

(ESA) recently announced the possible development of Seastar, which would provide ocean surface current vectors at 1 km resolution for the coastal ocean and shelf seas. Data from remotely-sensed space-born platforms, such as Seastar, present the best possibility for expanding the number of useable ocean current observations for ocean data assimilation and modeling.

Acknowledgments

This work was funded in part by the DARPA Ocean of Things program. This work is DoD Distribution Statement "A" (approved for public release, distribution unlimited).

References

Carrier, M. J., H. Ngodock, S. Smith, G. Jacobs, P. Muscarella, T. Ozgokmen, B. Haus, and B. Lipphardt, 2014: Impact of assimilating ocean velocity observations inferred from Lagrangian drifter data using the NCOM-4DVAR. *Mon. Wea. Rev.*, **142**, 1509-1524, doi:10.1175/MWR-D-13-00236.1.

Carrier, M. J., H. E. Ngodock, P. Muscarella, and S. Smith, 2016: Impact of assimilating surface velocity observations on the model sea surface height using the NCOM-4DVAR. *Mon. Wea. Rev.*, **144**, 1051-1068, doi:10.1175/MWR-D-14-00285.1.

Coelho, E. F., and Coauthors, 2015: Ocean current estimation using a multi-model ensemble kalman filter during the Grand Lagrangian Deployment experiment (GLAD). *Ocean Modell*., **87**, 86-106, doi:10.1016/j.ocemod.2014.11.001.

Davis, R. E., 1985: Drifter observations of coastal surface currents during CODE: The method and descriptive view. *J. Geophys. Res.: Oceans*, **90**, 4741-4755, doi:10.1029/JC090iC03p04741.

Fan, S., L.-Y. Oey, and P. Hamilton, 2004: Assimilation of drifter and satellite data in a model of the northeastern Gulf of Mexico. *Cont. Shelf Res*., **24**, 1001-1013, doi:10.1016/j.csr.2004.02.013.

Helber, R. W., T. L. Townsend, C. N. Barron, J. M. Dastugue, and M. R. Carnes, 2013: Validation test report for the Improved Synthetic Ocean Profile (ISOP) system, part 1: Synthetic profile methods and algorithm. NRL Internal Report, 128 pp, https://apps.dtic.mil/sti/pdfs/ADA585251.pdf.

Hernandez, F., P. Y. Le Traon, and N. H. Barth, 1995: Optimizing a drifter cast strategy with a genetic algorithm. *J. Atmos. Oceanic Technol.*, **12**, 330-345, doi:10.1175/1520-0426(1995)012<0330:OADCSW>2.0.CO;2.

Ide, K., L. Kuznetsov, and C. K. R. T. Jones, 2002: Lagrangian data assimilation for point vortex systems. *J. Turbul.,* **3**, doi:10.1088/1468-5248/3/1/053.

Ishikawa, Y., T. Awaji, K. Akimoto, and B. Qiu, 1996: Successive correction of the mean sea surface height by the simultaneous assimilation of drifting buoy and altimetric data. *J. Phys. Oceanogr*., **26**, 2381-2397, doi:10.1175/1520-0485(1996)026<2381:SCOTMS>2.0.CO;2.

Kuznetsov, L., K. Ide, and C. K. R. T. Jones, 2003: A method for assimilation of Lagrangian data. *Mon. Wea. Rev.*, **131**, 2247-2260, doi:10.1175/1520-0493(2003)131<2247:AMFAOL>2.0.CO;2.

Le Traon, P.-Y., and Coauthors, 2015: Use of satellite observations for operational oceanography: recent achievements and future prospects. *J. Oper. Oceanogr*., **8**, s12-s27, doi:10.1080/1755876X.2015.1022050.

Molcard, A., L. I. Piterbarg, A. Griffa, T.M. Ozgokmen, and A. J. Mariano, 2003: Assimilation of drifter positions for the reconstruction of the Eulerian circulation field. *J. Geophys. Res*., **108**, doi:10.1029/2001JC001240.

Molcard, A., A. Griffa, and T. M. Ozgokmen, 2005: Lagrangian data assimilation in multilayer primitive equation ocean models. *J. Atmos. Oceanic. Technol*., **22**, 70-83, doi:10.1175/JTECH-1686.1.

Muscarella, P., M. J. Carrier, H. Ngodock, S. Smith, B. L. Lipphardt Jr., A. D. Kirwan Jr., and H. S. Huntley, 2015: Do assimilated drifter velocities improve Lagrangian predictability in an operational ocean model? *Mon. Wea. Rev*., **143**, 1822-1832, doi:10.1175/MWR-D-14-00164.1.

Ngodock, H. E., and M. J. Carrier, 2014: A 4DVAR system for the Navy Coastal Ocean Model. Part I: System description and assimilation of synthetic observations in the Monterey Bay. *Mon. Wea. Rev*., **142**, 2085-2107, doi:10.1175/MWR-D-13-00221.1.

Nilsson, J. A. U., S. Dobricic, N. Pinardi, P.-M. Poulain, and D. Pettenuzzo, 2012: Variational assimilation of Lagrangian trajectories in the Mediterranean Ocean forecasting system. *Ocean. Sci*., **8**, 249-259, doi:10.5194/os-8-249-2012.

Ozgokmen, T. M., A. Molcard, T. M. Chin, L. I. Piterbarg, and A. Griffa, 2003: Assimilation of drifter positions in primitive equation models of midlatitude ocean circulation. *J. Geophys. Res: Oceans*., **108**, doi:10.1029/2002JC001719.

Phillipson, L., and R. Toumi, 2017: Impact of data assimilation on ocean current forecasts in the angola basin. *Ocean Modell.*, **114**, 45-58, doi:10.1016/j.ocemod.2017.04.006.

Phillipson, L., Y. Li, and R. Toumi, 2021: Strongly coupled assimilation of a hypothetical ocean current observing network within a regional ocean-atmosphere coupled model: An OSSE case study of Typhoon Hato. *Mon. Wea. Rev*., **149**, 1317-1336, doi:10.1175/MWR-D-20-0108.1.

Poje, A. C., and Coauthors, 2014: Submesoscale dispersion in the vicinity of the Deepwater Horizon spill. *Proc. Natl. Acad. Sci.*, **111**, 12693-12698, doi:10.1073/pnas.1402452111.

Powell, B., H. G. Arango, A. M. Moore, E. Di Lorenzo, R. F. Milliff, and D. Foley, 2008: 4DVAR data assimilation in the Intra-America Sea with the Regional Ocean Modeling System (ROMS). *Ocean Modell*., **23**, 130-145, doi:10.1016/j.ocemod.2008.04.008.

Santoki, M., S. Ratheesh, R. Sharma, K. N. Joshipura and S. Basu, 2012: Assimilation of drifter data in a circulation model of the Indian Ocean. *IEEE Geosci. Remote Sens. Lett.*, **9**, 100-103, doi:10.1109/LGRS.2011.2161455.

Smith, S. R., R. Helber, G. Jacobs, C. Barron, M. Carrier, C. Rowley, H. Ngodock, M. Yaremchuk, I. Pasmans, B. Bartels, and C. DeHaan, 2021: Ocean drifter velocity data assimilation Part 2: Prediction validation. In submission to *Ocean Modelling*.

Souopgui, I., J. M. D'Addezio, C. D. Rowley, S. R. Smith, G. A. Jacobs, R. W. Helber, M. Yaremchuk, J. J. Osborne, 2020: Multi-scale assimilation of simulated SWOT observations. *Ocean Modell*., **154**, doi:10.1016/j.ocemod.2020.101683.

Sun, L., and S. G. Penny, 2019: Lagrangian data assimilation of surface drifters in a double-gyre ocean model using the local ensemble transform Kalman filter. *Mon. Wea. Rev*., **147**, 4533-4551, doi:10.1175/MWR-D-18-0406.1.

Taillandier, V., A. Griffa, and A. Molcard, 2006: A variational approach for the reconstruction of regional scale Eulerian velocity fields from Lagrangian data. *Ocean Modell*., **13**, 1–24, doi:10.1016/j.ocemod.2005.09.002.

Toner, M., A. D. Kirwan Jr., L. H. Kantha, and J. K. Choi, 2001: Can general circulation models be assessed and their output enhanced with drifter data. *J. Geophys. Res: Oceans*., **106**, 19563-19579, doi:10.1029/2000JC000587.

Weaver, A. T., C. Deltel, E. Machu, S. Ricci, and N. Daget, 2005: A multivariate balance operator for variational ocean data assimilation. *Quart. J. Roy. Meteor. Soc*., **131**, 3605-3625, doi:10.1256/qj.05.119.

Yaremchuk, M., and A. Sentchev, 2011: A combined EOF/variational approach for mapping radar-derived sea surface currents. *Cont. Shelf Res*., **31**, 758-768, doi:10.1016/j.csr.2011.01.009.

Fine-scale structuring of open ocean ecosystems: From observations to management in a changing climate

Alice Della Penna[1], Camrin D. Braun[2], Peter Gaube[3], and Francesco dOvidio[5]

[1]University of Auckland, New Zealand
[2]Woods Hole Oceanographic Institution
[3]University of Washington
[4] Sorbonne Université, CNRS, IRD, MNHN, Laboratoire d'Océanographie et du Climat: Expérimentations et Approches Numériques (LOCEAN-IPSL), France

Marine ecosystems in a flowing medium

In recent years, studies of physical/biological interactions in the ocean have placed significant focus on processes occurring on spatial scales ranging from hundreds of meters to hundreds of kilometers. Research on these fine-scale features has revealed the role that mesoscale and submesoscale variability has in the distribution of heat, salt, and nutrients and how it can structure marine ecosystems.

Mesoscale eddies are geographically-balanced vortices, having typical sizes of 10-200 km and lifetimes from a few days to months, that can be observed using satellite altimetry and a host of other space-borne sensors. Coherent eddies can trap large parcels of water in their interiors and transport them over vast distances (Chelton et al. 2011a,b). Eddies and meanders also modulate vertical exchanges between ocean surface and interior (Gaube et al. 2014; McGillicuddy 2016) with observable impacts on primary production (Benitez-Nelson et al. 2007; Chelton et al. 2011a; Mahadevan et al. 2012; Lehahn et al. 2018), phytoplankton community composition (d'Ovidio et al. 2010; Clayton et al. 2013; Bolaños et al. 2020), and carbon biogeochemistry (Harrison et al. 2018).

High-resolution satellite images and numerical simulations have recently shed new light on ubiquitous, ageostrophic motion at the submesoscale (1-10 km, few hours to few days), including fronts, filaments, and vortices, and how they modulate life in the ocean (Lévy et al. 2014; Mahadevan 2016; Zhang and Qiu 2020). Of particular significance are the vertical fluxes associated with these transient submesoscale features that can be orders of magnitude larger than those resulting from basin and mesoscale variability (Klein and Lapeyre 2009; Lévy et al. 2012; Mahadevan, 2016; Rosso et al. 2016; Kessouri et al. 2020).

Challenges and limitations of current observations

Our understanding of these fine scale dynamics and associated ecological impacts are fundamentally shaped by the observations collected by satellite altimeters together with the analysis and synthesis of a multitude of remote and in situ observations and numerical simulation. Contemporary sea surface height observations can only resolve larger fine scale processes with minimum diameters of ~100 km at mid-latitudes (Chelton et al. 2011b; Ballarotta et al. 2019) and over-simplify the often-anisotropic shape of eddies (Amores et al. 2017). Features smaller than ~100 km are visible in high resolution images of sea surface temperature and ocean color. Unfortunately satellite imagery requires cloud-free conditions, resulting in sparse and largely unpredictable observations of submesoscale variability. As a result, repeated observations of submesoscale features are rare, inhibiting the ability to conduct extensive mechanistic and process-based studies at these scales. Thus, the current observational capacity leaves us unable to resolve many key pieces of the submesoscale regime, including measurements of vertical velocities in the water column, which are essential to quantify vertical nutrient fluxes (D'Asaro 2001).

In conjunction with limitations in observing fine scale variability of ocean circulation, difficulties in observing the distribution of different taxa and trophic levels leave many unanswered questions as to the mechanisms regulating phytoplankton community structure and secondary production. Growing global observing systems, like the fleet of autonomous floats built to sample phytoplankton biomass (Bio-Argo; Chai et al. 2020), have illuminated the complex interactions between phytoplankton bulk production and fine scale circulation. Yet, much less is known about the impact of fine scale currents on plankton community composition and diversity which generates more uncertainty in our capacity to model biogeochemical functions, particularly in a changing climate. Current observational studies will need to be extended to reach a comprehensive understanding of the impact of fine-scale dynamics on phytoplankton community composition, possibly integrating advanced analytical tools, like genomics, imaging, and optics (Sosik et al. 2007; Chase et al. 2017; Busseni et al. 2020; Bolaños et al. 2020).

The details of fine-scale biophysical coupling are even more uncertain for middle trophic levels. The few studies conducted on this topic suggest that the patchiness created by fine-scale currents impacts the distribution of zooplankton and micronekton (Sabarros et al. 2009; Bertrand et al. 2014; Baudena et al. 2021). This impact extends below the mixed layer to the mesopelagic ocean (Godø et al. 2012; Della Penna and Gaube 2020), the portion of the water column between 200-1000 m that has been estimated to host approximately 99% of the global fish biomass (Irigoien et al. 2014).

While it remains difficult to disentangle direct and indirect effects of fine-scale features across trophic levels, a growing body of research has shown that these processes clearly impact marine apex predators. For example, open-ocean fisheries have used satellite observations of fine-scale features for decades. Fishing vessels are known to congregate on fronts and at the peripheries of mesoscale eddies (Prants et al. 2014; Scales et al. 2018) which appears to be a cost-effective strategy for targeting commercially-valuable predator species (Watson et al. 2018) and may reflect how middle trophic levels (e.g., prey species) are impacted by fine-scale circulation processes (Baudena et al. 2021). While the focus has historically been on the presence/absence of predators at these features through analyses of catch and sightings data, a growing dataset of individual animal tracking data from marine mammals, sharks, turtles, and seabirds indicate that many predators preferentially occupy fronts, eddies, and meanders (Figure 1) (Cotté et al. 2007; Tew-Kai et al. 2009; Della Penna et al. 2015; Gaube et al. 2017; Gaube et al. 2018; Braun et al. 2019; Oliver et al. 2019). A few studies have explored the mechanisms driving these relationships and suggest they are complex and taxa-dependent and include trapping and retention of productive and prey-rich waters (Cotté et al. 2015), increased accessibility of prey caused by the unique conditions of fine-scale features (Braun et al. 2019), and the direct mechanical effect of ocean currents (Della Penna et al. 2015). However, most studies investigating the use of fine-scale features by apex predators and fishing vessels quantify association

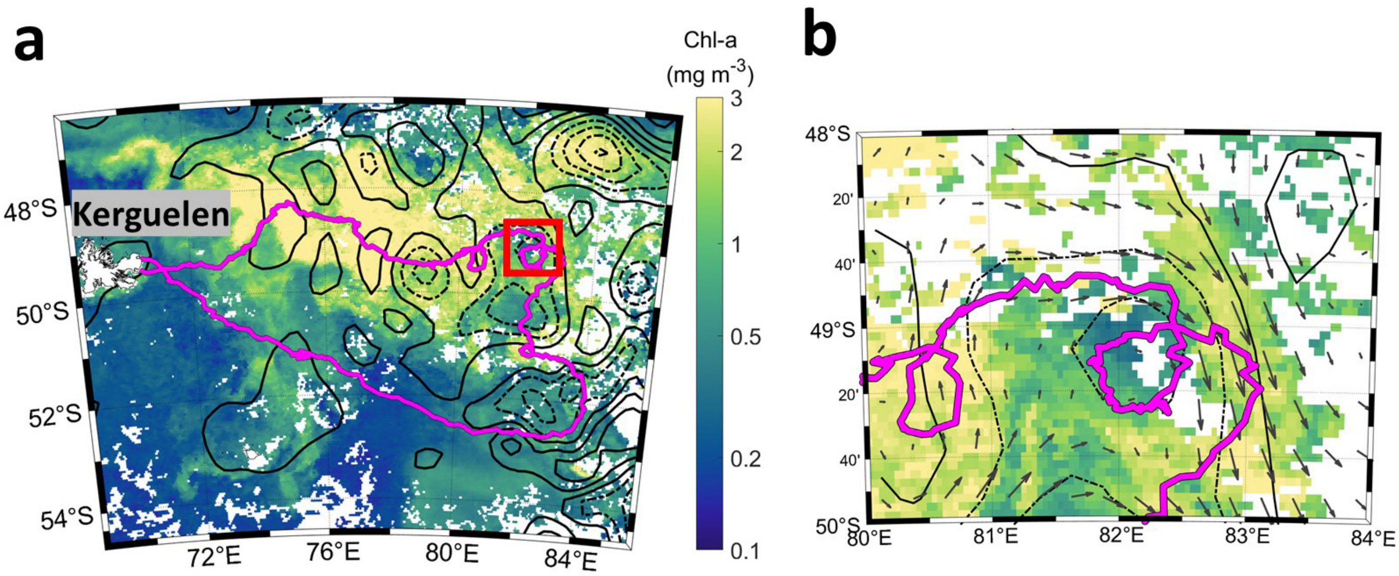

Figure 1. Trajectory of a foraging trip of a southern elephant seal (magenta) overlaid on composites of remotely-sensed near-surface chlorophyll-a (Chl-a). Black solid (dashed) contours indicate isolines of positive (negative) sea level anomaly (SLA) derived from satellite altimetry. The entire foraging trip lasted from November 2014 to February 2015. Subfigure (b) indicates a zoomed section of the trajectory in (a, red rectangle) corresponding to 1st December 2014. Chl-a composites were obtained by averaging daily maps over a 10 day period to mitigate the impact of cloud coverage. Grey arrows in (b) illustrate the geostrophic currents.

without detailed investigation of the mechanisms that modulate their utility to predators.

Expected improvements in observational capabilities of fine-scale physical/biological interactions

In the coming decade several new remote sensing tools are slated to become available that can help to investigate the multitude of existing and sure-to-come questions about fine scale variability of the ocean surface. The Surface Water and Ocean Topography satellite mission (SWOT, expected launch at the end of 2022) is expected to increase the resolution of altimetry-derived maps from ~100 km wavelength to 15-30 km, depending on the sea state (d'Ovidio et al., 2019; Morrow et al. 2019), opening a new window on the smallest mesoscale features and possibly allowing exploration of the impact of submesoscale processes on sea surface height. Observing smaller eddies that are not visible today, resolving the shape of larger eddies with the precision of a few kilometers, and better estimating fine-scale gradients are critical for advancing our understanding of biophysical processes. In particular, these advances will shed new light on the life cycle of fine-scale features, which are instrumental to reconstruct subsurface ocean dynamics (Pietri et al. 2021) and to properly co-locate physical features to biological data.

In parallel to advances in how we observe ocean circulation, the upcoming Plankton, Aerosol, Cloud, ocean Ecosystem mission (PACE, expected launch in late 2023) will put into orbit a hyperspectral radiometer to characterize the variability in light absorption and scattering, which can be linked to different phytoplankton groups. These measurements will provide valuable information about phytoplankton community composition that can currently only be observed in-situ (Ras et al. 2008; Chase et al. 2017) or estimated, with several limitations, from current ocean-color images (Mouw et al. 2017). Having high-resolution, high frequency, and extensive observations of phytoplankton community composition will increase our understanding of how ocean currents impact planktonic ecosystems and how such impact is reflected in carbon export and propagated up marine food webs.

In the coming decade spaceborne scatterometers that are able to measure ocean currents on 10 km scales over a ~1600 km swath (Rodriguez 2018) are also expected to revolutionize our understanding of fine scale dynamics. These measurements, that will not require the assumption of large-scale force balances as for altimetry, will be a valuable complement to SWOT and will move our understanding of the impact of fine-scale circulation on marine ecosystems even further into the ageostrophic, submesoscale regime.

A number of advances in in situ observing capabilities have also bolstered our ability to sense fine-scale physical and biological processes, including a variety of autonomous platforms and growing sensor networks. Miniaturisation of oceanographic-quality sensors has led to deployment on animals, which has become an essential component of an observing system tailored to physical/biological interactions. A growing library of data from animal-borne sensors has already dramatically improved sampling efforts, particularly in inaccessible environments such as polar seas (Fedak 2013; Treasure et al. 2017). These approaches have demonstrated the utility of sampling ocean processes at the fine-scale from the perspective of predators that presumably seek productive, small-scale features (Charrassin et al. 2008; Rivière et al. 2019) where important processes remain unresolved by current observing technologies (Siegelman et al. 2020). With a further miniaturization of sensors, cost reduction, and their broader deployment on marine animals, as well as integration with other in situ platforms, our capacity to characterize how different species and trophic levels interact with fine-scale oceanographic features will continue to grow.

Managing open ocean ecosystems in a changing climate

Open ocean ecosystems are notoriously difficult for spatial management (Hobday and Hartog 2014) despite their importance for a number of global processes, including feeding billions of people (Pauly et al. 2002; Game et al. 2009). Marine resource management has traditionally relied on fixed boundaries that reflect national or local jurisdictions. Yet these demarcations are of little relevance in an inherently dynamic ocean where many animals routinely make trans-boundary movements (Campana 2016; Della Penna et al. 2017). Thus, understanding fine-scale biophysical interactions is critical for managing marine ecosystems (Della Penna et al. 2017), especially in a rapidly changing climate.

As of 2021, only 7.7% of the ocean is protected and less than 3% is fully or highly protected (https://www.protectedplanet.net; Kriegl et al. 2021). These numbers are expected to grow dramatically in this decade, aiming at an ambitious 30% for both by 2030. In order to achieve this, an international, legally binding instrument (so called "Biodiversity Beyond National Jurisdiction") is being negotiated to extend the UN Convention on the Law of the Sea. This tool will provide a much needed juridical framework to regulate and enforce conservation measures in the vast areas of the open ocean outside national jurisdictions. Identifying the structural and functional role(s) of fine-scale features in marine ecosystems provides the opportunity for adaptive spatial management strategies including dynamic Marine Protected Areas that use a suite of ocean observing tools to account for a range of dynamic oceanographic processes (Hazen et al. 2018). Ultimately, the future of understanding, managing, and conserving living marine resources relies on a comprehensive understanding and improved predictability of the ocean at fine scales and its impact on marine ecosystems to dynamically optimize management based on the ever-changing marine environment (Maxwell et al. 2015).

Acknowledgments
We would like to thank Jennie Zhu, Kyla Drushka, and Mark Bourassa for the invitation to write this manuscript. The marine mammal data were collected and made freely available by the International MEOP Consortium and the

national programs that contribute to it. This study used satellite products distributed by E.U. Copernicus Marine Service Information and from the Ocean Colour Climate Change Initiative dataset, Version 5, European Space Agency, available online at http://www.esa-oceancolour-cci.org/. CDB and PG were supported by the NASA New Investigator Program 80NSSSC20K1132, and CDB was also supported by the NASA Earth Science Research Program 80NSSC19K0187.

References

Amores, A., S. Monserrat, O. Melnichenko, and N. Maximenko, 2017: On the shape of sea level anomaly signal on the periphery of mesoscale ocean eddies. *Geophys. Res. Lett*., **44**, 6926-6932, doi:10.1002/2017GL073978.

Ballarotta, M., and Coauthors, 2019: On the resolutions of ocean altimetry maps. *Ocean Sci.*, **15**, 1091-1109, doi:10.5194/os-15-1091-2019.

Baudena, A., E. Ser-Giacomi, D. D'Onofrio, X. Capet, C. Cotté, Y. Cherel, and F. d'Ovidio, 2021: Fine-scale structures as spots of increased fish concentration in the open ocean. *Sci. Rep.*, **11**, 1-13, doi:10.1038/s41598-021-94368-1.

Benitez-Nelson, C. R., and Coauthors, 2007: Mesoscale eddies drive increased silica export in the subtropical Pacific Ocean. *Science*, **316**, 1017-1021, doi:10.1126/science.1136221.

Bertrand, A., and Coauthors, 2014: Broad impacts of fine-scale dynamics on seascape structure from zooplankton to seabirds. *Nat. Commun.*, **5**, 1-9, doi:10.1038/ncomms6239.

Bolaños, L. M., and Coauthors, 2020: Small phytoplankton dominate western North Atlantic biomass. *ISME J.*, **14**, 1663-1674, doi:10.1038/s41396-020-0636-0.

Braun, C. D., P. Gaube, T. H. Sinclair-Taylor, G. B. Skomal, and S. R. Thorrold, 2019: Mesoscale eddies release pelagic sharks from thermal constraints to foraging in the ocean twilight zone. *Proc. Natl. Acad. Sci.*, **116**, 17187-17192, doi:10.1073/pnas.1903067116.

Busseni, G., and Coauthors, 2020: Large scale patterns of marine diatom richness: Drivers and trends in a changing ocean. *Global Ecol. Biogeogr.*, **29**, 1915-1928, doi:10.1111/geb.13161.

Campana, S. E., 2016: Transboundary movements, unmonitored fishing mortality, and ineffective international fisheries management pose risks for pelagic sharks in the Northwest Atlantic. *Can. J. Fish. Aquat. Sci.,* **73**, doi:10.1139/cjfas-2015-0502.

Chai, F., and Coauthors, 2020: Monitoring ocean biogeochemistry with autonomous platforms. *Nat. Rev. Earth Environ.*, **1,** 315–326, doi:10.1038/s43017-020-0053-y.

Charrassin, J. B., and Coauthors, 2008: Southern Ocean frontal structure and sea-ice formation rates revealed by elephant seals. *Proc. Natl. Acad. Sci.*, **105**, 11634-11639, doi:10.1073/pnas.0800790105.

Chase, A. P., E. Boss, I. Cetinić, and W. Slade, 2017: Estimation of phytoplankton accessory pigments from hyperspectral reflectance spectra: Toward a global algorithm. *J. Geophys. Res. Oceans*, **122**, 9725-9743, doi:10.1002/2017JC012859.

Chelton, D. B., M. G. Schlax, and R. M. Samelson, 2011b: Global observations of nonlinear mesoscale eddies. *Prog. Oceanogr.*, **91**, 167-216, doi:10.1016/j.pocean.2011.01.002.

Chelton, D. B., P. Gaube, M. G. Schlax, J. J. Early, and R. M. Samelson, 2011a: The influence of nonlinear mesoscale eddies on near-surface oceanic chlorophyll. *Science*, **334**, 328-332, doi:10.1126/science.1208897.

Clayton, S., S. Dutkiewicz, O. Jahn, and M. J. Follows, 2013: Dispersal, eddies, and the diversity of marine phytoplankton. *Limnol. Oceanogr.: Fluids Environ.*, **3**, 182-197, doi:10.1215/21573689-2373515.

Cotté, C., F. d'Ovidio, A. C.Dragon, C. Guinet, and M. Lévy, 2015: Flexible preference of southern elephant seals for distinct mesoscale features within the Antarctic Circumpolar Current. *Prog. Oceanogr.*, **131**, 46-58, doi:10.1016/j.pocean.2014.11.011.

Cotté, C., Y. H. Park, C. Guinet, and C. A. Bost, 2007: Movements of foraging king penguins through marine mesoscale eddies. *Proc. Roy. Soc. B.*, **274**, 2385-2391, doi:10.1098/rspb.2007.0775.

D'Asaro, E. A., 2001: Turbulent vertical kinetic energy in the ocean mixed layer. *J. Phys. Oceanogr.*, **31**, 3530-3537, doi:10.1175/1520-0485(2002)031<3530:TVKEIT>2.0.CO;2.

d'Ovidio, F., and Coauthors, 2019: Frontiers in fine-scale in situ studies: Opportunities during the swot fast sampling phase. *Front. Mar. Sci.*, **6**, doi:10.3389/fmars.2019.00168.

d'Ovidio, F., S. De Monte, S. Alvain, Y. Dandonneau, and M. Lévy, 2010: Fluid dynamical niches of phytoplankton types. *Proc. Natl. Acad. Sci.*, **107**, 18366-18370, doi:10.1073/pnas.1004620107.

Della Penna, A., and P. Gaube, 2020: Mesoscale eddies structure mesopelagic communities. *Front. Mar. Sci.,* **7**, doi:10.3389/fmars.2020.00454.

Della Penna, A., P. Koubbi, C. Cotté, C. Bon, C. A. Bost, and F. d'Ovidio, 2017: Lagrangian analysis of multi-satellite data in support of open ocean Marine Protected Area design. *Deep Sea Res. Part II*, **140**, 212-221, doi:10.1016/j.dsr2.2016.12.014.

Della Penna, A., S. De Monte, E. Kestenare, C. Guinet, and F. d'Ovidio, 2015: Quasi-planktonic behavior of foraging top marine predators. *Sci. Rep.*, **5**, 1-10, doi:10.1038/srep18063.

Fedak, M. A., 2013: The impact of animal platforms on polar ocean observation. *Deep Sea Res. Part II*, **88-89**, 7-13, doi:10.1016/j.dsr2.2012.07.007.

Game E. T., and Coauthors, 2009: Pelagic protected areas: The missing dimension in ocean conservation. *Trends Ecol. Evol.,* **24**, 360–369, doi:10.1016/j.tree.2009.01.011.

Gaube, P., C. Barceló, D. J. McGillicuddy, A. Domingo, P. Miller, B. Giffoni, N. Marcovaldi, and Y. Swimmer, 2017: The use of mesoscale eddies by juvenile loggerhead sea turtles (*Caretta caretta*) in the southwestern Atlantic. *PloS One*, **12**, doi:10.1371/journal.pone.0172839.

Gaube, P., C. D. Braun, G. L. Lawson, D. J. McGillicuddy, A. Della Penna, G. B. Skomal, C. Fischer, and S. R. Thorrold, 2018: Mesoscale eddies influence the movements of mature female white sharks in the Gulf Stream and Sargasso Sea. *Sci. Rep.*, **8**, doi:10.1038/s41598-018-25565-8.

Gaube, P., D. J. McGillicuddy, D. B. Chelton, M. J. Behrenfeld, and P. G. Strutton, 2014: Regional variations in the influence of mesoscale eddies on near-surface chlorophyll. *J. Geophys. Res.: Oceans*, **119**, 8195-8220, doi:10.1002/2014JC010111.

Godø, O. R., A. Samuelsen, G. J. Macaulay, R. Patel, S. S. Hjøllo, J. Horne, S. Kaartvedt, and J. A. Johannessen, 2012: Mesoscale eddies are oases for higher trophic marine life. *PloS One*, **7**,doi:10.1371/journal.pone.0030161.

Harrison, C. S., M. C. Long, N. S. Lovenduski, and J. K. Moore, 2018: Mesoscale effects on carbon export: A global perspective. *Global Biogeochem. Cycles*, **32**, 680-703, doi:10.1002/2017GB005751.

Hazen, E. L., and Coauthors, 2018: A dynamic ocean management tool to reduce bycatch and support sustainable fisheries. *Sci. Adv.*, **4**, doi:0.1126/sciadv.aar3001.

Hobday A. J., and J. R. Hartog, 2014: Derived ocean features for dynamic ocean management. *Oceanography,* **27**, 134–145, doi:10.5670/oceanog.2014.92.

Irigoien, X., and Coauthors, 2014: Large mesopelagic fishes biomass and trophic efficiency in the open ocean. *Nat. Commun.*, **5**, doi:10.1038/ncomms4271.

Kessouri, F., D. Bianchi, L. Renault, J. C. McWilliams, H. Frenzel, and C. A. Deutsch, 2020: Submesoscale currents modulate the seasonal cycle of nutrients and productivity in the California Current system. *Global Biogeochem. Cycles*, **34**, doi:10.1029/2020GB006578.

Klein, P., and G. Lapeyre, 2009: The oceanic vertical pump induced by mesoscale and submesoscale turbulence. *Annu. Rev. Mar. Sci.*, **1**, 351-375, doi:10.1146/annurev.marine.010908.163704.

Kriegl, M., X. E. Elías Ilosvay, C. von Dorrien, and D. Oesterwind, 2021: Marine protected areas: At the crossroads of nature conservation and fisheries management. *Front. Mar. Sci.*, **8**, doi:10.3389/fmars.2021.676264.

Lehahn, Y., F. d'Ovidio, and I. Koren, 2018: A satellite-based Lagrangian view on phytoplankton dynamics. *Annu. Rev. Mar. Sci.,* **10**, 99-119, doi:10.1146/annurev-marine-121916-063204.

Lévy, M., O. Jahn, S. Dutkiewicz, and M. J. Follows, 2014: Phytoplankton diversity and community structure affected by oceanic dispersal and mesoscale turbulence. *Limnol. Oceanogr.*, **4**, 67-84, doi:10.1215/21573689-2768549.

Lévy, M., R. Ferrari, P. J. Franks, A. P. Martin, and P. Rivière, 2012: Bringing physics to life at the submesoscale. *Geophys. Res. Lett*., **39**, doi:10.1029/2012GL052756.

Mahadevan A., 2016: The impact of submesoscale physics on primary productivity of plankton. *Annu. Rev. Mar. Sci.,* **8**, 161–184, doi:annurev-marine-010814-015912.

Mahadevan, A., E. D'asaro, C. Lee, and M. J. Perry, 2012: Eddy-driven stratification initiates North Atlantic spring phytoplankton blooms. *Science*, **337**, 54-58, doi:10.1126/science.1218740.

Maxwell, S. M., and Coauthors, 2015: Dynamic ocean management: Defining and conceptualizing real-time management of the ocean. *Mar. Policy*, **58**, 42-50, doi:10.1016/j.marpol.2015.03.014.

McGillicuddy, D. J., 2016: Mechanisms of physical-biological-biogeochemical interaction at the oceanic mesoscale. *Annu. Rev. Mar. Sci.*, **8**, 125-159, doi:10.1146/annurev-marine-010814-015606.

Morrow, R., and Coauthors, 2019: Global observations of fine-scale ocean surface topography with the Surface Water and Ocean Topography (SWOT) mission. *Front. Mar. Sci.*, **6**, doi:10.3389/fmars.2019.00232.

Mouw, C. B., and Coauthors, 2017: A consumer's guide to satellite remote sensing of multiple phytoplankton groups in the global ocean. *Front. Mar. Sci.*, **4**, doi:10.3389/fmars.2017.00041.

Oliver, M. J., and Coauthors, 2019: Central place foragers select ocean surface convergent features despite differing foraging strategies. *Sci. Rep.,* **9**, doi:10.1038/s41598-018-35901-7.

Pauly D., V. Christensen, S. Guénette, T. J. Pitcher, U. Rashid Sumaila, C. J. Walters, R. Watson, and D. Zeller, 2002: Towards sustainability in world fisheries. *Nature*, **418**, 689–695, doi:10.1038/nature01017.

Pietri, A., X. Capet, F. d'Ovidio, M. Levy, J. Le Sommer, J. M. Molines, and H. Giordani, 2021: Skills and limitations of the adiabatic omega equation: How effective is it to retrieve oceanic vertical circulation at mesoscale and submesoscale?. *J. Phys. Oceanogr.*, **51**, 931-954, doi:10.1175/JPO-D-20-0052.1.

Prants, S. V., M. V. Budyansky, and M. Y. Uleysky, 2014: Identifying Lagrangian fronts with favourable fishery conditions. *Deep Sea Res. Part* I, **90**, 27-35, doi:10.1016/j.dsr.2014.04.012.

Ras, J., H. Claustre, and J. Uitz, 2008: Spatial variability of phytoplankton pigment distributions in the Subtropical South Pacific Ocean: Comparison between in situ and predicted data. *Biogeosciences*, **5**, 353-369, doi:10.5194/bg-5-353-2008.

Rivière P., T. Jaud, L. Siegelman, P. Klein, C. Cotté, J. Le Sommer, G. Dencausse, and C. Guinet, 2019: Sub-mesoscale fronts modify elephant seals foraging behavior. *Limnol. Oceanogr. Lett.*, **4**, 193–204, doi:10.1002/lol2.10121.

Rodriguez, E., 2018: On the optimal design of Doppler scatterometers. *Remote Sens.,* **10**, doi:10.3390/rs10111765.

Rosso, I., A. M. Hogg, R. Matear, and P. G. Strutton, 2016: Quantifying the influence of sub-mesoscale dynamics on the supply of iron to Southern Ocean phytoplankton blooms. *Deep Sea Res. Part I*, **115**, 199-209, doi:10.1016/j.dsr.2016.06.009.

Sabarros, P. S., F. Ménard, J. J. Lévénez, E. Tew-Kai, and J. F. Ternon, 2009: Mesoscale eddies influence distribution and aggregation patterns of micronekton in the Mozambique Channel. *Mar. Ecol. Prog. Ser.*, **395**, 101-107, doi:10.3354/meps08087.

Scales, K. L., E. L. Hazen, M. G. Jacox, F. Castruccio, S. M. Maxwell, R. L. Lewison, and S. J. Bograd, 2018: Fisheries bycatch risk to marine megafauna is intensified in Lagrangian coherent structures. *Proc. Natl. Acad. Sci.*, **115**, 7362-7367, doi:10.1073/pnas.1801270115.

Siegelman L., P. Klein, P. Rivière, A. F. Thompson, H. S. Torres, M. Flexas, and D. Menemenlis, 2020: Enhanced upward heat transport at deep submesoscale ocean fronts. *Nat. Geosci.*, **13**, 50–55, doi:10.1038/s41561-019-0489-1.

Sosik, H. M., and R. J. Olson, 2007: Automated taxonomic classification of phytoplankton sampled with imaging-in-flow cytometry. *Limnol. Oceanogr. Lett.*, **5**, 204-216, doi:10.4319/lom.2007.5.204.

Tew Kai, E., V. Rossi, J. Sudre, H. Weimerskirch, C. Lopez, E. Hernandez-Garcia, F. Marsac, and V. Garçon, 2009: Top marine predators track Lagrangian coherent structures. *Proc. Natl. Acad. Sci.*, **106**, 8245-8250, doi:10.1073/pnas.0811034106.

Treasure, A. M., and Coauthors, 2017: Marine mammals exploring the oceans pole to pole: A review of the MEOP consortium. *Oceanography*, **30**, 132-138, doi:10.5670/oceanog.2017.234.

Watson, J. R., E. C. Fuller, F. S. Castruccio, and J. F. Samhouri, 2018: Fishermen follow fine-scale physical ocean features for finance. *Front. Mar. Sci.*, **5**, doi:10.3389/fmars.2018.00046.

Zhang, Z., and B. Qiu, 2020: Surface chlorophyll enhancement in mesoscale eddies by submesoscale spiral bands. *Geophys. Res. Lett.*, **47**, doi:10.1029/2020GL088820.

ANNOUNCEMENTS

Nominate an Early Career Scientist

The US CLIVAR Early Career Scientist Leadership Awards seek to recognize early career members of the US Earth system science community for their contributions to leading community activities to advance science on the role of the ocean in climate variability and predictability. Leadership can take many forms, and this award opportunity allows for highlighting such diversity in making impactful contributions to community activities.

Propose a new Working Group

The US CLIVAR program establishes limited-lifetime, action-oriented Working Groups of scientists to coordinate and implement focused activities for the benefit of the scientific community. Working Groups supported from this year's call will be initiated by Spring 2022 and undertake actionable and measurable tasks over a 2–3 year period.

Apply to serve on a US CLIVAR Panel

The US CLIVAR Panels formulate science goals and implementation strategies, catalyze and coordinate activities, and work with agencies and international partners to advance the progress of the climate research community. Each Panel is seeking members to enhance current strengths while adding expertise in new areas.

Deadlines

Early Career Scientist Leadership Award nominations: October 15, 2021

Working Group requests: October 15, 2021

Panel member applications: October 29, 2021

usclivar.org
uscpo@usclivar.org
twitter.com/usclivar

US Climate Variability and Predictability (CLIVAR) Program
Washington, DC 20005

US CLIVAR acknowledges support from these US agencies:

This material was developed with federal support of NASA (80NSSC17M0007), NOAA (NA11OAR4310213), NSF (AGS-1502208), and DOE (DE-SC0016332). Any opinions, findings, conclusions, or recommendations expressed in this material are those of the authors and do not necessarily reflect the views of the sponsoring agencies.